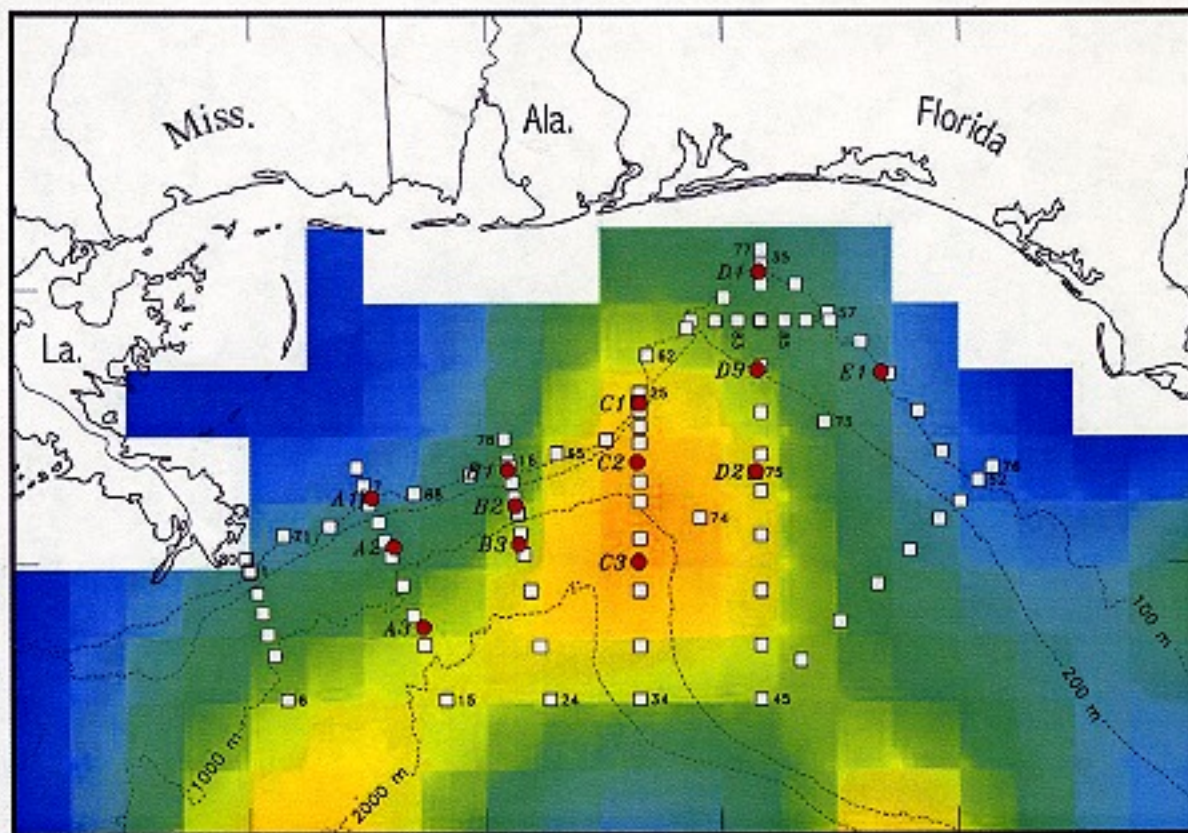


DeSoto Canyon Eddy Intrusion Study

Final Report

Volume I: Executive Summary



DeSoto Canyon Eddy Intrusion Study

Final Report

Volume I: Executive Summary

Authors

Thomas J. Berger
Peter Hamilton
James J. Singer
Evans Waddell
Science Applications International Corporation

James H. Churchill
Woods Hole Oceanographic Institute

Robert R. Leben
University of Colorado

Thomas N. Lee
University of Miami

Wilton Sturges
Florida State University

Prepared under MMS Contract
1435-01-96-CT-30825
by
Science Applications International Corporation
615 Oberlin Rd., Suite 300
Raleigh, North Carolina 27605

Published by

U.S. Department of the Interior
Minerals Management Service
Gulf of Mexico OCS Region

New Orleans
November 2000

DISCLAIMER

This report was prepared under contract between the Minerals Management Service (MMS) and Science Applications International Corporation (SAIC). This report has been technically reviewed by the MMS and approved for publication. Approval does not signify that the contents necessarily reflect the views and policies of the Service, nor does mention of trade names or commercial products constitute endorsement or recommendation for use. It is, however, exempt from review and compliance with the MMS editorial standards.

REPORT AVAILABILITY

Extra copies of the report may be obtained from the Public Information Office (Mail Stop 5034) at the following address:

U.S. Department of the Interior
Minerals Management Service
Gulf of Mexico OCS Region
Public Information Office (MS 5034)
1201 Elmwood Park Boulevard
New Orleans, Louisiana 70123-2394

Telephone Number: 1-800-200-GULF or
504-736-2519

CITATION

Suggested Citation:

Hamilton, P., T.J. Berger, J.J. Singer, E. Waddell, J.H. Churchill, R.R. Leben, T.N. Lee, and W. Sturges. DeSoto Canyon Eddy Intrusion Study; Final Report Volume I: Executive Summary. OCS Study MMS 2000-079. U.S. Dept. of the Interior, Minerals Management Service, Gulf of Mexico OCS Region, New Orleans, LA. 37 pp.

ABOUT THE COVER

The map of the northeastern Gulf of Mexico on the cover of this report shows the locations of moorings (red dots) and hydrographic stations (white squares) occupied during the DeSoto Canyon Eddy Intrusion Study. These locations are overlaid on a color-coded map of sea surface height (SSH) as determined from satellite altimetry. The warmer colors (yellow/orange) indicate a higher SSH. This grades through green to blue in going to lower SSH. Note the horizontal scale of the yellow/orange colored feature that was centered among the moorings. Such a relative high is associated with anticyclonic (clockwise rotating) surface currents.

ACKNOWLEDGEMENTS

The Program Manager wishes to extend thanks to the captain and crew of the *R/V Pelican* for their continued support and conscientious effort during the many cruises conducted during the study. During data processing, Paul Blankinship provided excellent data processing and analysis support to the program principal investigators. Carol Harris did an outstanding job in the general production of this and many other project reports. For the duration of the program, Sharon Goodhart provided administrative and project support that has been key to the successful and timely completion of the study.

The continuing, enthusiastic and timely support of Dr. Alexis Lugo-Fernandez, the MMS Contract Officer's Technical Representative, during all phases of this project is gratefully acknowledged.

TABLE OF CONTENTS

VOLUME I

	<u>PAGE</u>
ACKNOWLEDGEMENTS.....	v
LIST OF FIGURES.....	ix
LIST OF TABLES.....	xi
1.0 INTRODUCTION.....	1
1.1 Background.....	1
1.2 Project Objectives.....	2
2.0 MEASUREMENTS AND OBSERVATIONS.....	5
2.1 Methods.....	5
3.0 LOOP CURRENT DYNAMICS.....	11
3.1 Introduction.....	11
3.2 LC Metrics and Statistics.....	11
3.3 LC Energetics and Dynamics.....	14
3.3.1 Introduction.....	14
3.3.2 Ring Separations.....	14
3.3.3 LC Forcing by the Wind Curl.....	17
4.0 SLOPE CIRCULATION PATTERNS.....	21
4.1 Introduction.....	21
4.2 Types and Sources of Eddy Influences.....	21
4.2.1 Loop Current Frontal Eddies.....	21
4.2.2 Cyclonic and Anticyclonic Eddies.....	29
4.2.3 Mean and Varying Circulation Patterns.....	29
4.2.4 Slope Dynamics and Fluxes.....	33
4.2.5 Deep Currents.....	33
5.0 ATMOSPHERIC FORCING.....	35
5.1 Synoptic Scale Forcing.....	35
5.2 Seasonal Wind Response on the Slope.....	35
5.3 Canyon Response to Hurricanes.....	36
5.4 Non-hurricane Inertial Currents.....	39
6.0 SUMMARY.....	41

LIST OF FIGURES

<u>Figure No.</u>	<u>Caption</u>	<u>Page</u>
1.1-1.	Image showing contours of sea surface height with examples of the types and scales of eddy-like features that can occur in the eastern and northeastern Gulf of Mexico.	2
1.2-1.	Base map of the study area with color coded image of the height of the sea surface (warmer colors are higher/taller) as determined by satellite altimeter.	3
2.1-1	Map showing standard hydrographic grid for the DeSoto Canyon Eddy Intrusion Study with feature survey stations for December 1998 cruise (Stations 81-87) and all 13 current meter mooring locations	6
2.1-2a.	Timeline of data return by instrument level for the indicated DeSoto Canyon Eddy Intrusion Study moorings	8
2.1-2b.	Timeline of data return by instrument level on indicated moorings for the DeSoto Canyon Eddy Intrusion Study.	9
3.2-1a.	Time series of Loop Current area, volume, and circulation for 1/1/1993 through 4/30/1999.	12
3.2-1b.	Time series of Loop Current northward and westward penetration, and length for 1/1/1993 through 4/30/1999.	13
3.2-2.	Percent occurrence of LC waters for the interval from 1/1/1993 through 4/30/1999.	15
3.2-3.	Mean SSH for the interval from April 1997 to April 1998.	16
3.3-1.	Periodicity of ring separations from the Loop Current.	18
3.3-2.	Power spectra of the north-south motion of the Loop Current and of wind stress curl over the full Gulf of Mexico.	19
3.3-3.	Cross spectra between the wind curl and Loop Current variability.	20

LIST OF FIGURES (continued)

<u>Figure No.</u>	<u>Caption</u>	<u>Page</u>
4.2-1.	SST image for April 12, 1998 (0247 CST).....	22
4.2-2.	Conceptual model of a Loop Current frontal eddy flow interaction with the slope in the study region.	24
4.2-3.	SST image for April 30, 1997 (1355 CST).....	25
4.2-4.	Conceptual model of flow interaction with the slope in the study region from a lcfw on the boundary of a warm LC ring.	26
4.2-5.	Conceptual model of flow interaction with the slope from a Loop Current frontal eddy close to the study region.	27
4.2-6.	Conceptualization of flow interaction with the slope from a Loop Current frontal eddy on the boundary of a warm LC ring located west of the Miss. delta and blocked by the Loop Current.	28
4.2-7.	Geostrophic velocities at 6m from the hydrographic surveys..	30
4.2-8.	Geostrophic velocities on Section B for the indicated surveys..	31
4.2-9.	Seven-DLP current vectors and isotherm depths for the upper 300m of C2.	32
5.3-1.	Comparison of inertial current magnitudes seen near the surface at moorings C3, D2 and E1 during late summer-early autumn 1998	37
5.3-2.	Surface wind stress together with near-bottom and near-surface inertial current magnitude observed at the indicated moorings over the study period.	38

LIST OF TABLES

<u>Table No.</u>	<u>Caption</u>	<u>Page</u>
3.2-1.	Statistics for Loop Current metrics (1/1/1993 - 4/30/1999)	14

1. INTRODUCTION

1.1 Background

The DeSoto Canyon Eddy Intrusion Study will provide the Minerals Management Service (MMS) with information and analysis which expands the understanding of physical oceanographic conditions and processes in the northeastern Gulf of Mexico. In turn, these insights will support an enhanced basis for developing sound, rationally based environmental assessments. The threat of a spill contacting land in the northeastern Gulf of Mexico is of great concern to the MMS. To estimate the potential for such a spill coming into contact with resources in the region, a robust "climatological" circulation, which includes the means and dominant oceanographic phenomena is needed. On the northeastern Gulf slope, Loop Current (LC) and eddy intrusions are two important processes to be included in any climatological circulation characterization of the area (see Figure 1.1-1 as an example).

To gather the data needed to assemble the oceanographic climatological database for oil spill trajectory analysis, the MMS funded the present DeSoto Canyon Eddy Intrusion Study. Knowledge acquired through this study will facilitate MMS's understanding of the outer shelf circulation, e.g., how the LC and associated eddies exchange momentum and mass with the shelf. The role of the DeSoto Canyon as a route that facilitates these intrusions and as a conduit of mass exchange between the deep gulf and the shelf will be further elucidated by characterizing processes and conditions over the adjacent slope. As described below, results and data from this study will also be useful to other concurrent oceanographic studies that the MMS and others are sponsoring in the northeastern Gulf.

1.2 Project Objectives

The general objectives of this study are:

- Use *in-situ* current measurements, hydrographic data, and satellite images to document and characterize LC intrusions and interactions with the northeastern Gulf slope (Figure 1.2-1, for illustration). This study shall examine the frequency and horizontal and vertical extent of these interactions and intrusions. Through the use of dynamical principles, a conceptual model will be used to help explain the character and evolution of LC-slope interactions observed in the course of the study.
- Document and examine the dynamical processes of momentum, mass and vertical vorticity exchanges occurring during LC-slope interactions. These analyses shall be based on the *in-situ* current measurements and hydrographic data.
- Estimate the frequency of LC, LC rings and secondary eddies' interactions with the northeastern slope, and conduct an assessment of the vertical and horizontal shears, exchanges of vorticity, momentum, and mass fields associated with the eddy-slope interactions.

Gulf of Mexico Sea Surface Height

TOPEX/ERS-2 sea surface height anomaly
plus 10-year climatological model mean

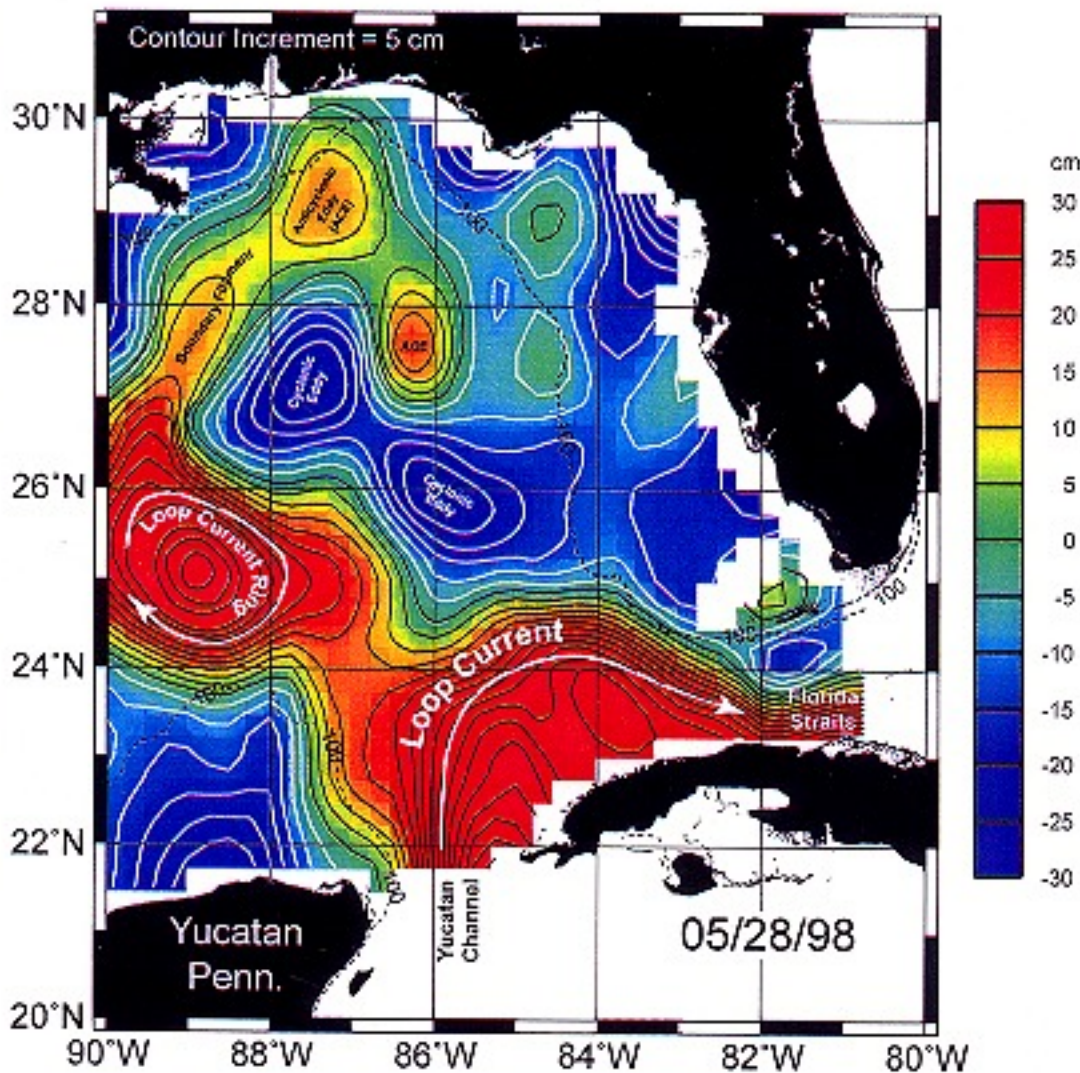


Figure 1.1-1. Image showing contours of sea surface height with examples of the types and scales of eddy-like features that can occur in the eastern and northeastern Gulf of Mexico. The eastern and northeastern Gulf can have a "rich" and dynamic eddy field.

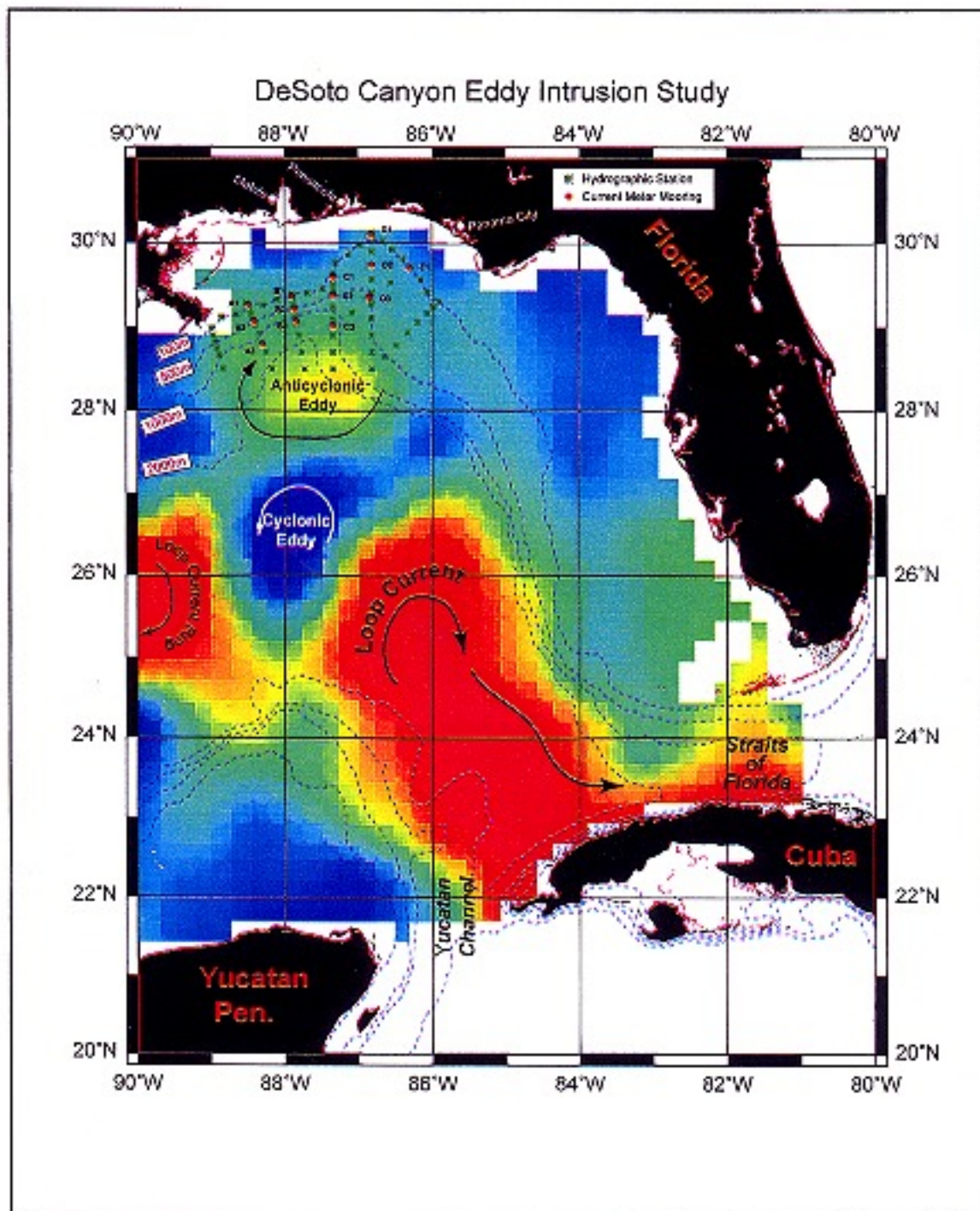


Figure 1.3-1. Base map of the study area with color coded image of the height of the sea surface (warmer colors are higher/taller) as determined by satellite altimeter. Several key oceanographic features are labeled. On the slope (seaward of 100m isobath) off Alabama and the Florida Panhandle are shown the locations of current meter moorings and hydrographic stations occupied during the DeSoto Canyon Eddy Intrusion Study.

- Elucidate the role of the DeSoto Canyon in LC and eddy processes as a mechanism and as well as a route of mass and momentum exchange between the shelf and deep water of the northeastern Gulf.

The overall program was to last 4 years with two complete years of field observations in the general study area (Figure 1.2-1). The general location and configuration of moorings were specified in the Scope of Work provided by the MMS. The general area for the hydrographic sampling scheme was also specified. SAIC proposed some limited modifications that were incorporated into the overall design that produced the observational database used for this report. It is important to note that several concurrent and complementary programs involving physical oceanographic measurements were conducted in this general study area. The MMS is funding Texas A&M University to conduct a study titled "Northeastern Gulf of Mexico Chemical Oceanography and Hydrography Study" (Contract No. 1435-01-97-CT-30851). Additionally, selected physical oceanographic measurements are being made in the pinnacle area near and at the shelf break offshore of Alabama as part of an NBR/USGS-funded study being conducted by Continental Shelf Associates (CSA).

Members of the program's scientific team (Principal Investigators - PIs) and their primary areas of investigation on this project are presented below in alphabetical order:

- James Churchill (Woods Hole Oceanographic Institute - WHOI) - Canyon processes; atmospheric forcing due to hurricanes; shelf-slope exchange processes.
- Peter Hamilton (Science Applications International Corporation - SAIC) - Slope eddy dynamics; scales of motion; atmospheric forcing.
- Robert Leben (University of Colorado - UCol) - Loop Current, dynamics and metrics, ringshedding patterns and characteristics.
- Thomas Lee (University of Miami - UMiami) - Slope eddy kinematics; shelf-slope exchange processes and mechanisms.
- Wilton Sturges (Florida State University - FSU) - LC and LC ring dynamics.

An important support function was provided by James Singer (SAIC) who was responsible for the planning and conduct of all field operations and logistics and served as Program Chief Scientist on all cruises. Throughout most of the program, Thomas J. Berger was the Program Manager. Although recently retired, he was responsible for the oversight and guidance of activities during all but the creation of this final report.

2.0 MEASUREMENTS AND OBSERVATIONS

2.1 Methods

The DeSoto Canyon Eddy Intrusion Study involved acquisition and use of a broad range of ocean and remotely sensed measurements over a two-year field season. Measurements were begun on March 18, 1997 and completed on approximately April 6, 1999. Field activities were conducted during seven mooring maintenance and hydrographic cruises conducted approximately every four months over the two-year interval. Types of field measurements included:

In-situ observations

- Current velocities using normal current meters that measure velocity and temperature at the level of the instrument (Figure 2.1-1);
- Acoustic Doppler current profiler (ADCP) which use a transmitted acoustic signal to estimate current velocities over a range of depths above the transducer,
- Stand alone thermistor that record temperature time series at positions between other instruments;
- Conductivity/temperature sensors that can with data conversion provide time series estimates of temperature and salinity; and

Ship-based survey observations

As part of the seven ship surveys, profiles of conductivity (salinity) and temperature were measured over a repeated grid of stations (Figure 2.1-1). It was also during these cruises that drifters were often released. To supplement the regular grid hydrography taken during the seven cruises, two special studies/surveys were conducted to help resolve finer scale features that may occur over the slope in the study area.

Remotely sensed (satellite-based) observations

An important element in reaching the goal of this program was access to remotely sensed sea surface temperature (SST) and sea surface height (SSH) observations. A multi-spectral radiometer on a polar orbiting satellite provided observations that were calibrated to estimate the temperature of the sea surface (skin) temperature. Given a clear sky (no clouds to intercept the thermal radiation), this provides at least twice daily essentially instantaneous SST patterns in the eastern Gulf of Mexico. When ocean surface temperature gradients exist (nominally October - May) SST patterns help identify evolving surface current patterns. The MMS has a contract with the US Geological Survey (USGS) to provide, via the Internet, navigated and calibrated images of SST in the eastern Gulf. These images are publicly accessible at:

http://coastal.er.usgs.gov/east_gulf/html/sst.html

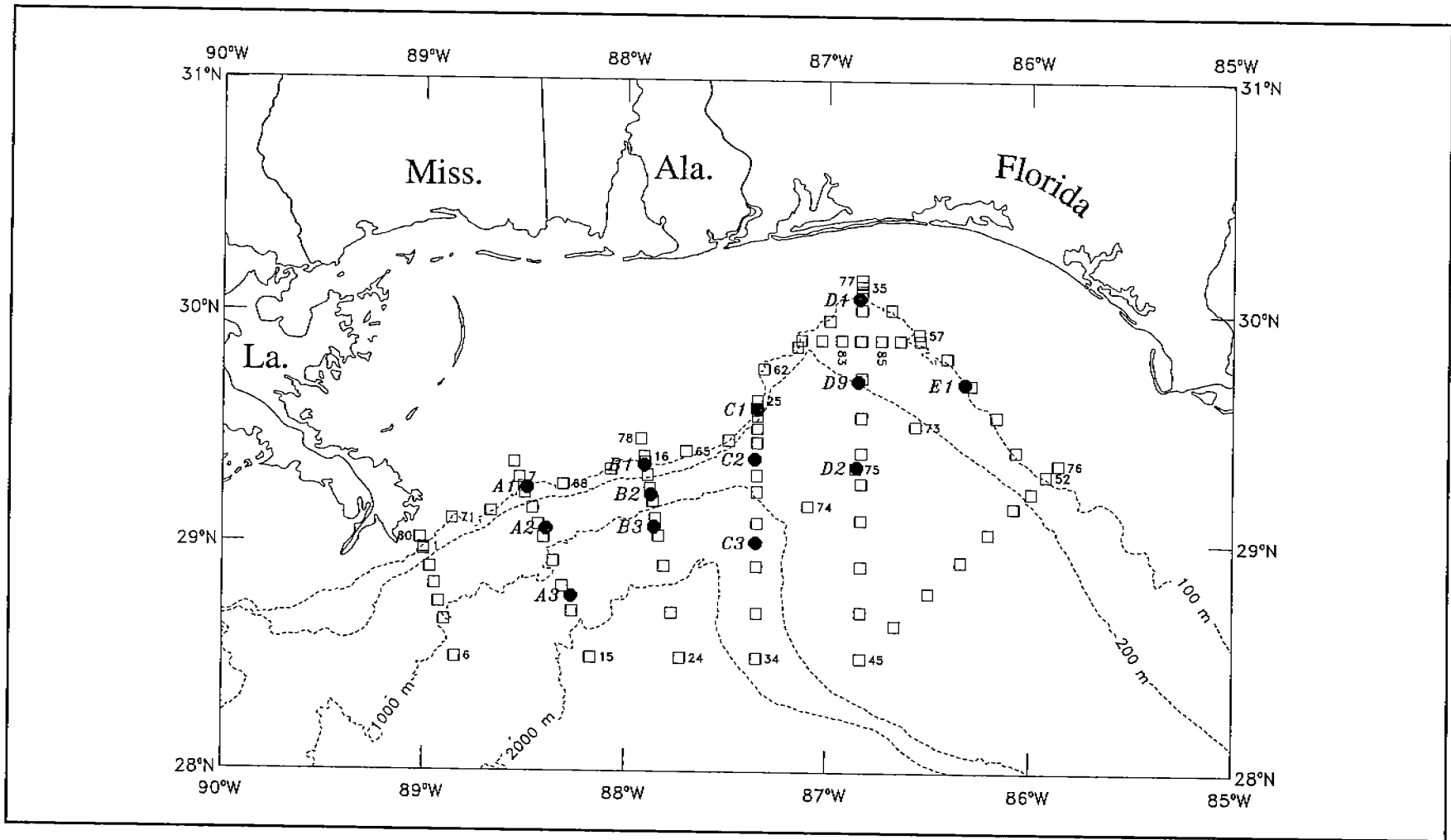


Figure 2.1-1 Map showing standard hydrographic grid for the DeSoto Canyon Eddy Intrusion Study with feature survey stations for December 1998 cruise (Stations 81-87) and all 13 current meter mooring locations (solid circles).

SSH data are provided by at least two satellites having different coverage patterns and schedules. The resulting altimetry database has been integrated into an estimate of the Gulf-wide pattern of SSH. This methodology, which has been evaluated against actual sea surface current patterns (e.g. drifting buoy trajectories) is best left for description in the main body of this report. Suffice it to say, the data processing scheme produces a once a day estimate of the SSH. Using these height estimate, the pattern and magnitude of pressure driven (geostrophic) surface currents can be estimated. These SSH images are publicly available from the following Internet site:

<http://www-ccar.colorado.edu/~realtime/gom/gom.html>.

The processing of the altimetry as well as maintenance of this Internet site were and are being done by the Colorado Center for Astrodynamics Research (CCAR) at the University of Colorado, one of the participants in this project.

Lagrangian observations

- Drifters that move with the ambient surface currents and periodically report their positions via a satellite link.

All the above types observations are supplemented by environmental observations being made and reported routinely by NOAA/NWS and NOAA/NDBC, such as coastal and at-sea wind velocity, and air and water temperatures, hurricane trajectories and characteristics and coastal sealevel.

As illustrated in the project time lines (Figures 2.1-2a,b), excellent data return was maintained by the field measurement program. As a result, a comprehensive multivariate data set was available to the program Principal Investigators to help reach the program's goal of describing oceanographic features and processes occurring over the continental slope in the oceanographically complex DeSoto Canyon region of the NE Gulf of Mexico.

Measurement Timeline DeSoto Canyon Eddy Intrusion Study

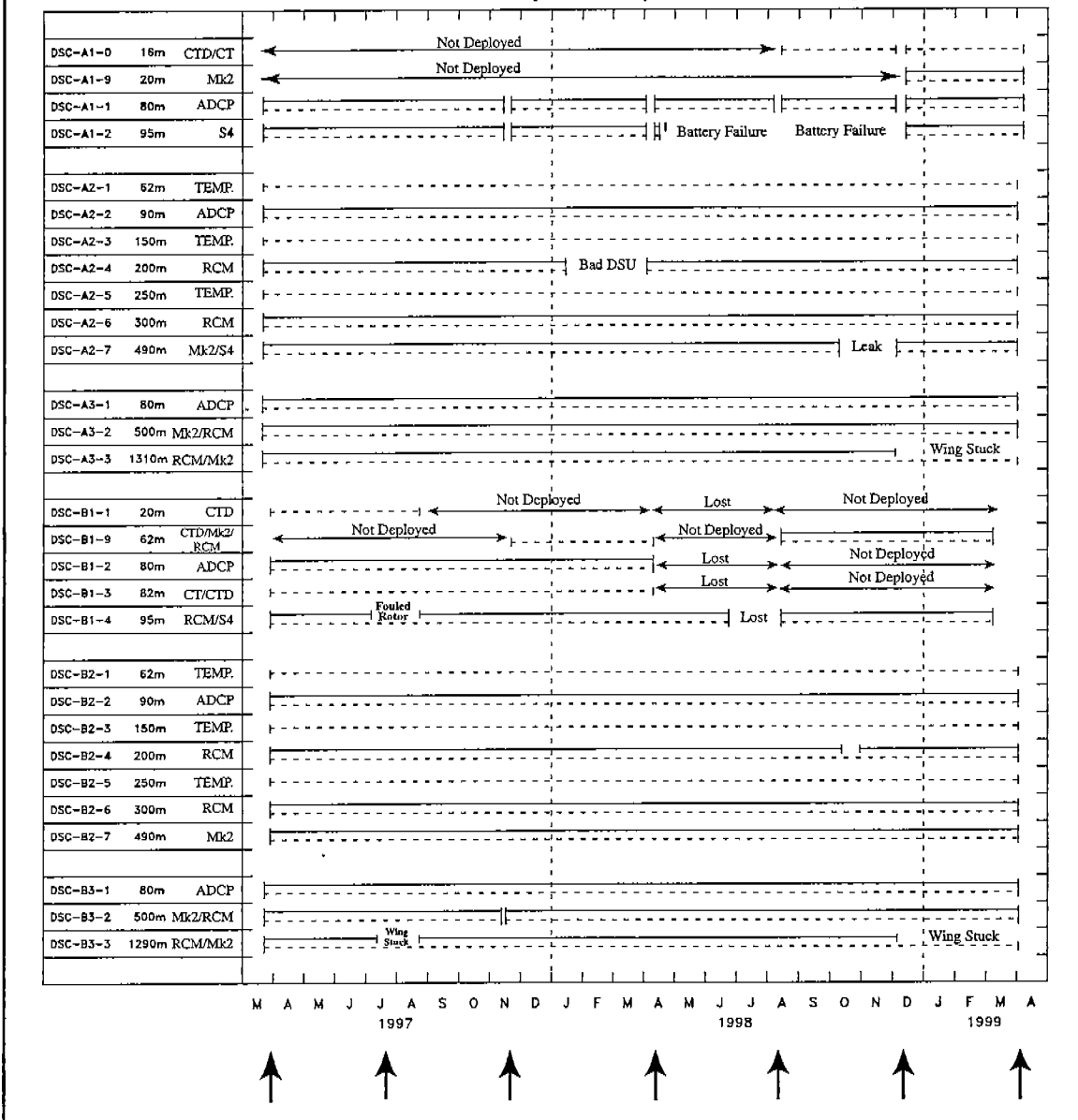


Figure 2.1-2a. Timeline of data return by instrument level on the indicated DeSoto Canyon Eddy Intrusion Study moorings. Arrows indicate the approximate dates of the hydrographic cruises.

Measurement Timeline DeSoto Canyon Eddy Intrusion Study

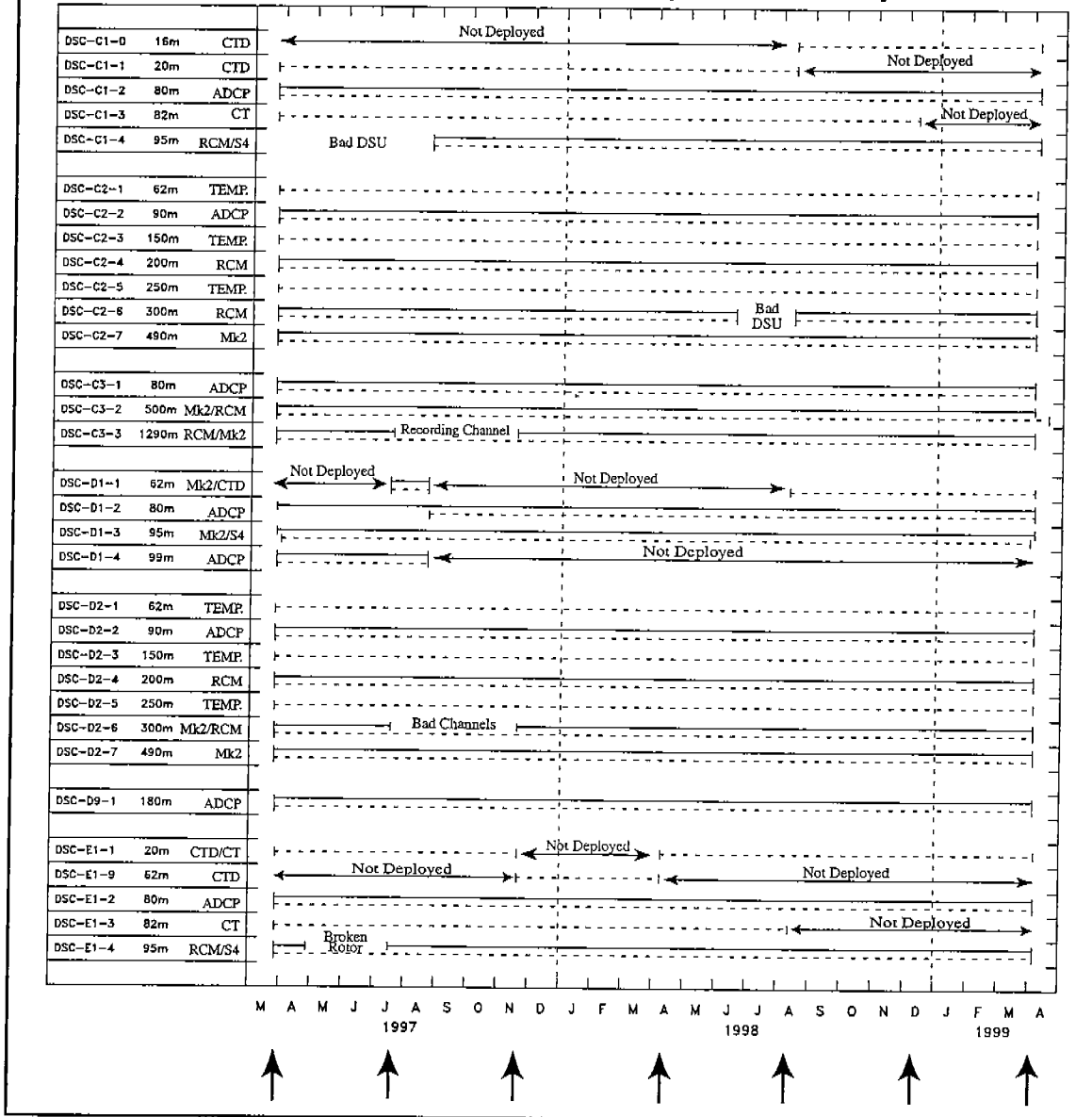


Figure 2.1-2b. Timeline of data return by instrument level on the indicated moorings for the DeSoto Canyon Eddy Intrusion Study. Arrows indicate the approximate dates of the hydrographic cruises.

3.0 LOOP CURRENT DYNAMICS

3.1 Introduction

The Loop Current (LC) and related processes are key source of energy and momentum for circulation features in the NE Gulf of Mexico. With this as background, a concerted effort was made to develop a comprehensive description of the morphology (boundary length, enclosed area, etc.) of the LC, the recent history of change associated with ring shedding and some of the dynamics associated with ring assimilation into Gulf waters.

3.2 LC Metrics and Statistics.

A variety of LC metrics and statistics were computed using SSH information. To facilitate joint use of data sets a comparison was made of the LC frontal boundary location as estimated by SST imagery and the location of the 17 cm SSH contour. These two methods of estimating LC position were generally in good agreement, however, the 17 cm height contour was consistently south of the SST front by about 1° of latitude or approximately 100 km. This is consistent with other definitions of the LC and LC ring boundaries as estimated by subsurface temperature structure. Often the location of the primary current field associated with the LC and LC rings is defined as where the 15°C isotherm drops below 200m depth. This location will also consistently be south (inside) of the location of the surface thermal front. Note that the 17 cm height contour usually enters the Gulf through the Yucatan Channel, follows the LC boundary and exits the Gulf through the Straits of Florida.

Shown in Figure 3.2-1a,b are time series of LC area, LC volume, maximum northward LC intrusion, maximum westward LC intrusion and length of the LC. The occurrence of ring shedding events has been indicated so this influence can readily be identified. Over the six years available for examination with these techniques, the length of the LC varied between slightly less than 800 km and approximately 2300 km - a change of almost 300% with a time mean length of 1390 km. Ring shedding events caused length reductions of between 600 km and 1100 km. Using the 17 cm height contour, the maximum northern and western excursions were 27.5°N and 90°W respectively. The most southern and eastern maximum excursions were approximately 24°N and 86°W. These latter "lesser" maximums immediately followed a ring separation. LC area varied between 0.8 - 1.9 x 10⁵ km² with a mean area of 1.4 x 10⁵ km². The range of area would have been less and the mean area larger but for shedding of two large rings. Some of these statistics are summarized in Table 3.2-1 (4.2-1). An examination of the time series shown in the Figure 3.2-1 panels, suggests the strong correlation between these variables. Computations of correlations showed a minimum coefficient of 0.82 between any of these descriptive variables.

To help provide an understanding of when and where LC water may be found, the percent occurrence has been mapped and contoured (Figure 3.2-2). As expected, LC water occurs at more northerly positions less often than positions to the south. This drawing also provides an impression for the general shapes that the LC assumes as it grows from the most

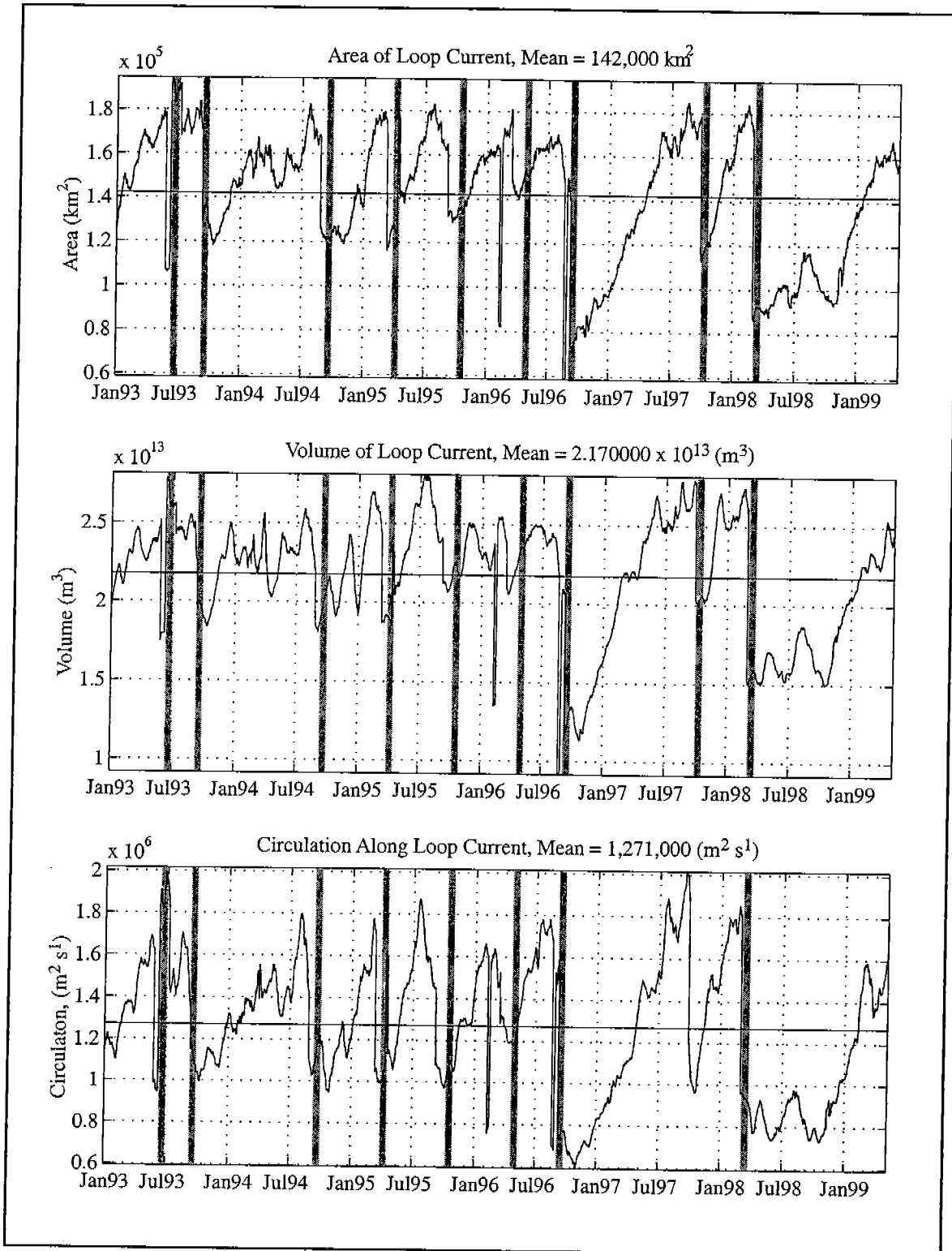


Figure 3.2-1a. Time series of Loop Current area, volume, and circulation for 1/1/1993 through 4/30/1999. Ring shedding events are shown by vertical gray lines.

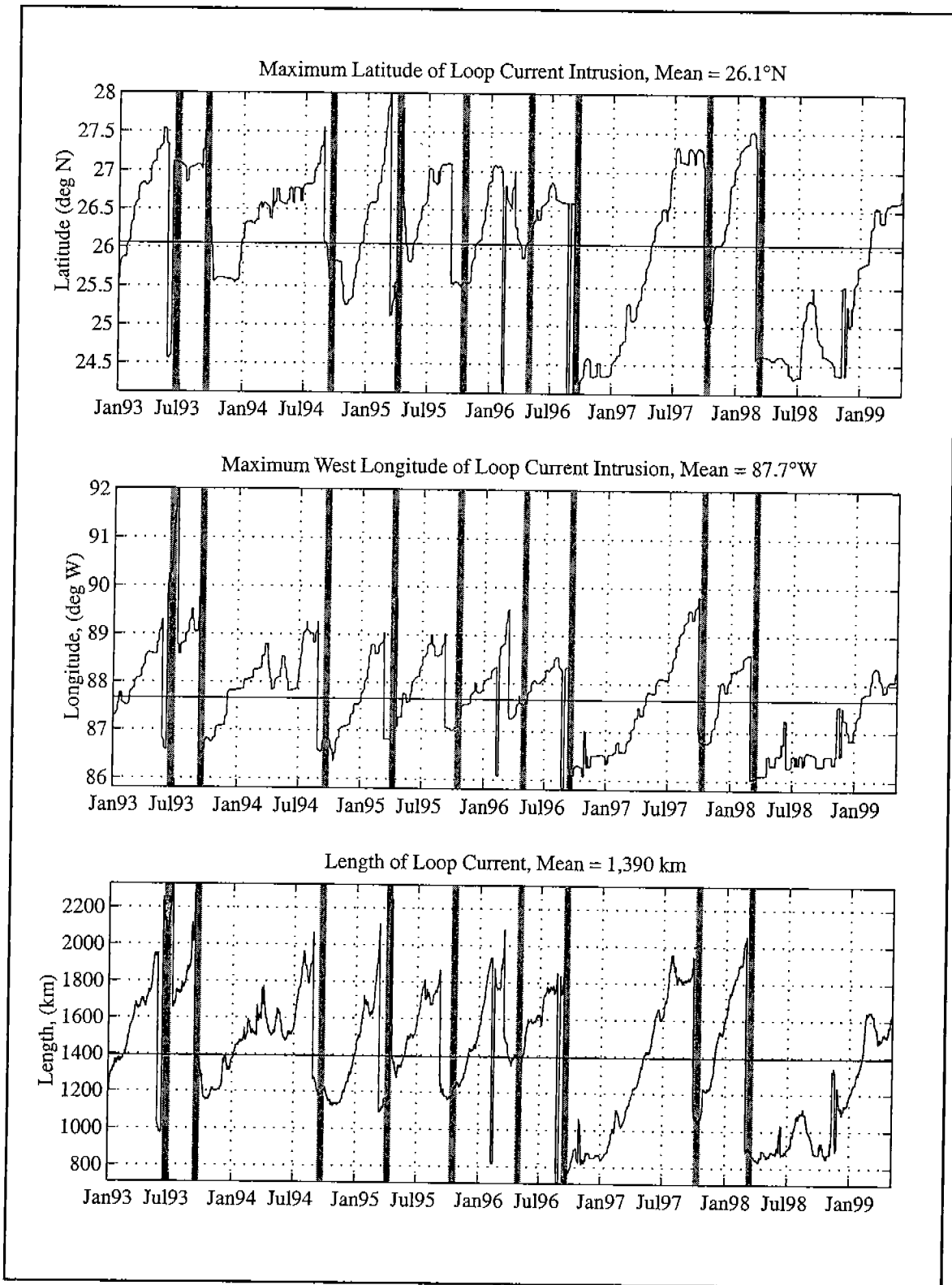


Figure 3.2-1b. Time series of Loop Current northward and westward penetration, and length for 1/1/1993 through 4/30/1999. Ring shedding events are shown by vertical gray lines.

southerly position following ring shedding to a more northerly and westerly position expected prior to shedding. A contour map of the mean SSH fields during this project are shown in Figure 3.2-3.

3.3 LC Energetics and Dynamics

3.3.1 Introduction

Because LC ring shedding is one of the most important and dynamic events in the Gulf of Mexico, an effort was made as part of this program to understand the dynamic magnitude of the process. It should be noted that access to remotely sensed SSH observations were an important contributor to this line of investigation.

Table 3.2-1. Statistics for Loop Current Metrics (1/1/1993 -4/30/1999).

	West Longitude	North Latitude	Length	Area	Volume	Circulation
Mean	87.7°W	26.1°N	1390 km	142,000 km ²	2.17x10 ¹³ m ³	1,271,000 m ² /sec
Std. Dev.	0.97°	0.93°	321 km	28,300 km ²	0.37x10 ¹³ m ³	321,190 m ² /sec
Maximum	92.0°W	28.0°N	2016 km	194,600 km ²	2.81x10 ¹³ m ³	2,016,200 m ² /sec
Minimum	85.8°W	24.1°N	593 km	58,600 km ²	0.91x10 ¹³ m ³	593,480 m ² /sec

3.3.2 Ring Separations

To understand the ring shedding process, an historical perspective is essential. Over the years a number of investigators have looked at the ring shedding cycle (interval between shedding events). With availability of SSH information, in particular for the summer months when SST imagery provides minimal information, the prior estimates of ring shedding can be expanded confidently. Figure 3.3-1 (4.3-1) shows a smoothed frequency plot - actually a manipulated relative frequency plot - showing separations since 1973.

In a geophysical context where ring shedding may be linked to the larger basin-scale patterns having decadal time scales, ring shedding cycles of approximately one year as measured over 25 years may be misleading. The proper time scale for evaluation of confidence may be such that only two or three cycles of basin-scale patterns may have occurred over the 25 years of ring shedding information. Regardless, the data in Figure 3.3-1 shows that the most noticeable region of power is near one year - 11.6 months - but specifically not at one year. The mean value, for 33 separation intervals in 313 months is near 9.5 months, although there is little power at this period. The absence of power at the mean is neither surprising nor unusual for events having a range of values such as these separation intervals.

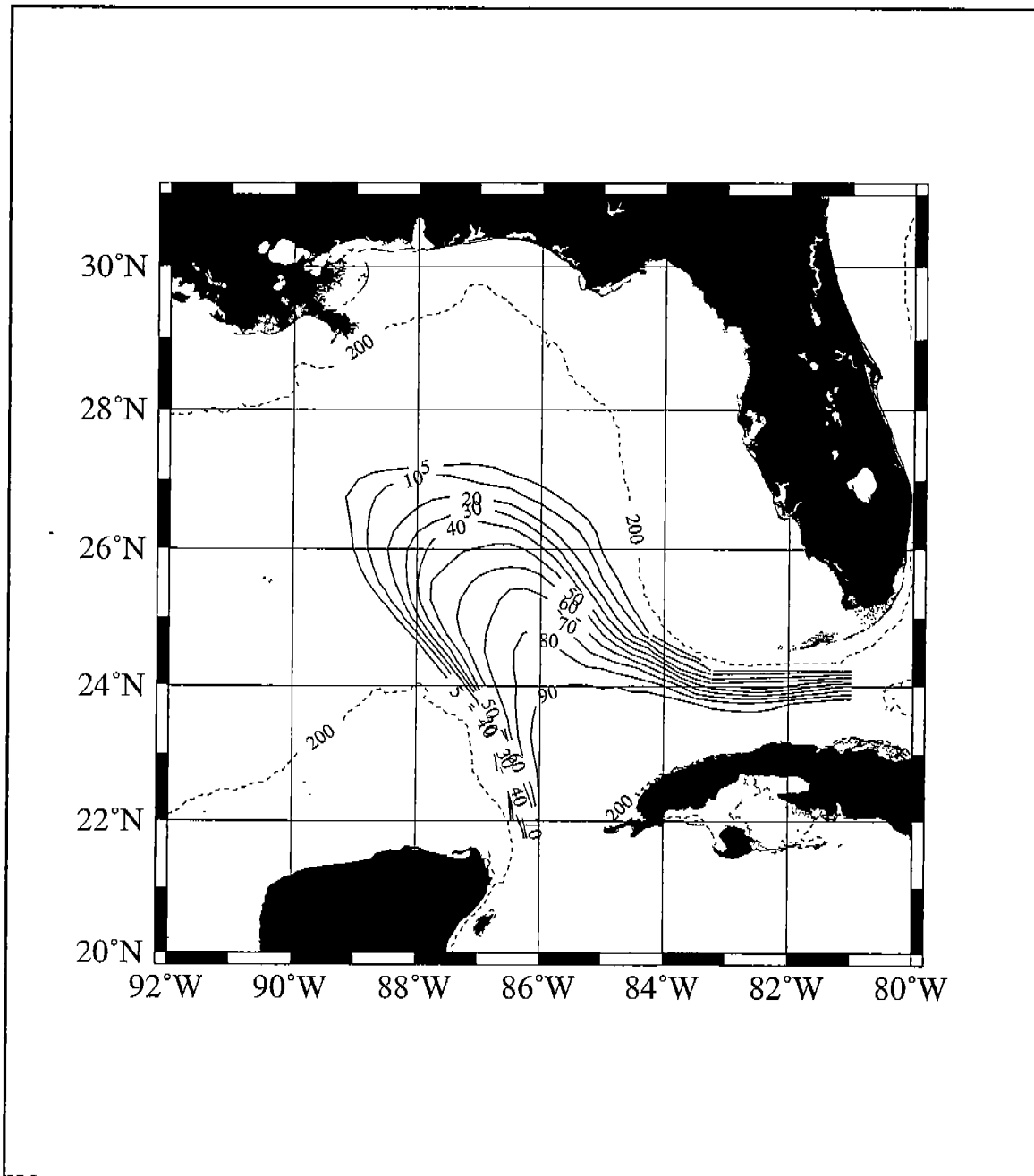


Figure 3.2-2. Percent occurrence of LC waters for the interval from 1/1/1993 through 4/30/1999.

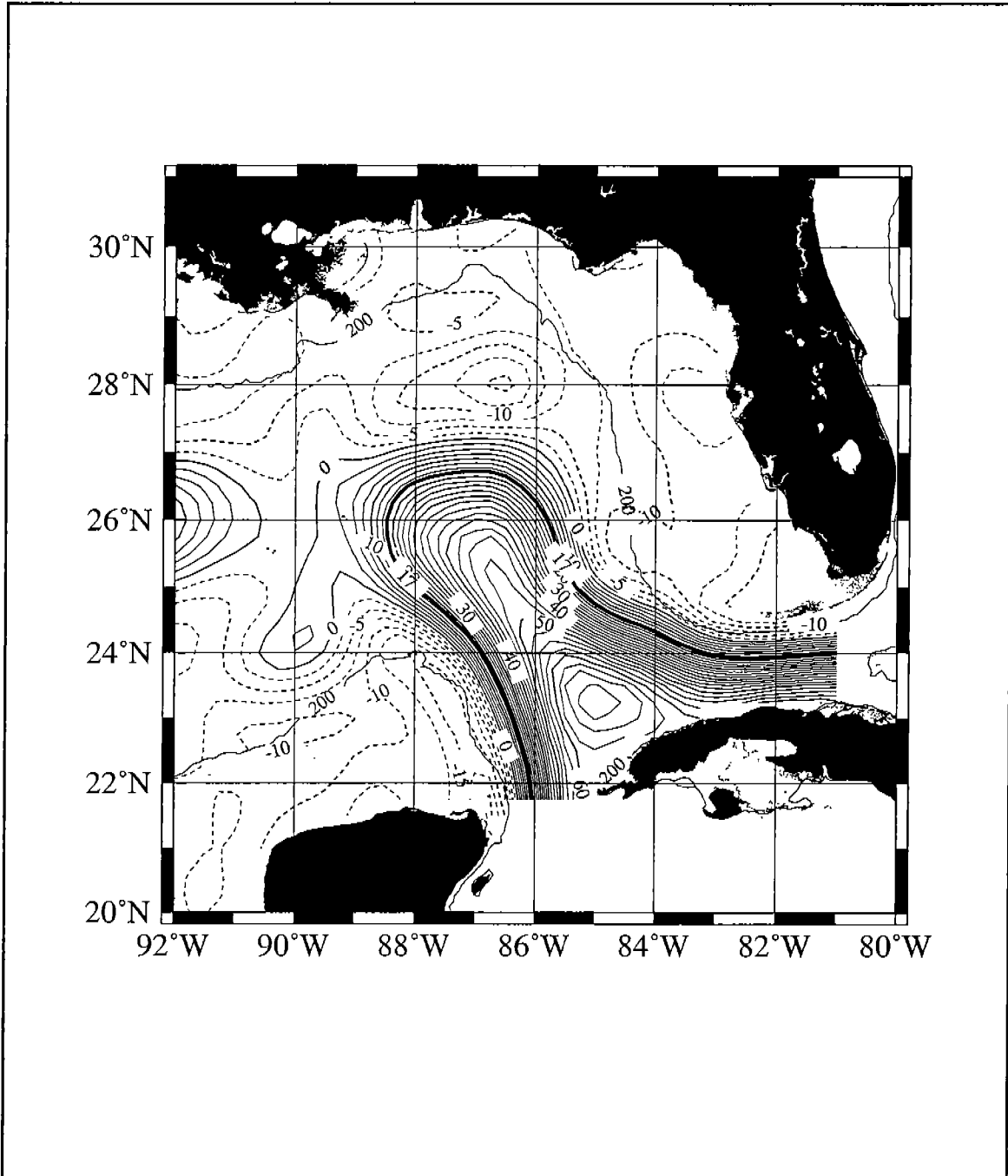


Figure 3.2-3. Mean SSH for the interval from April 1997 to April 1998.

3.3.3 LC Forcing by the Wind Curl

The premise of this section is that most of the Gulf of Mexico is forced downward by Ekman pumping and that this fluid volume is compensated by the upper-layer fluid displaced by the advancing LC front. It is suggested that the fluid that is thus pumped downward, on a time scale of decades eventually leaves *beneath* the incoming LC at depths below the main thermocline.

An order-of-magnitude analysis of the Ekman pumping by the wind curl shows that the work required to force a given volume of upper-layer fluid down through the known stratification of the Gulf is comparable to the available energy from work done by winds on the surface of the Gulf. This quantity agrees with the available potential energy of a LC ring. Consequently, on an annual basis the work done by the wind is sufficient to force down the volume of one ring per year.

An examination of the LC position (north-south) and the wind stress curl is shown in Figure 3.3-2. The coherence and phase of the two signals is shown in Figure 3.3-3. The strong coherence and appropriate phase relations provide additional support for the possible role of Ekman pumping and LC dynamics.

The various calculations and comparisons suggest a possible relationship between LC ring shedding and the curl of the wind stress over the Gulf of Mexico. This relationship is not "proven," rather the patterns and magnitudes of dynamic variables are such that they suggest such a relationship may exist. Further study is needed to evaluate and possibly show this linkage.

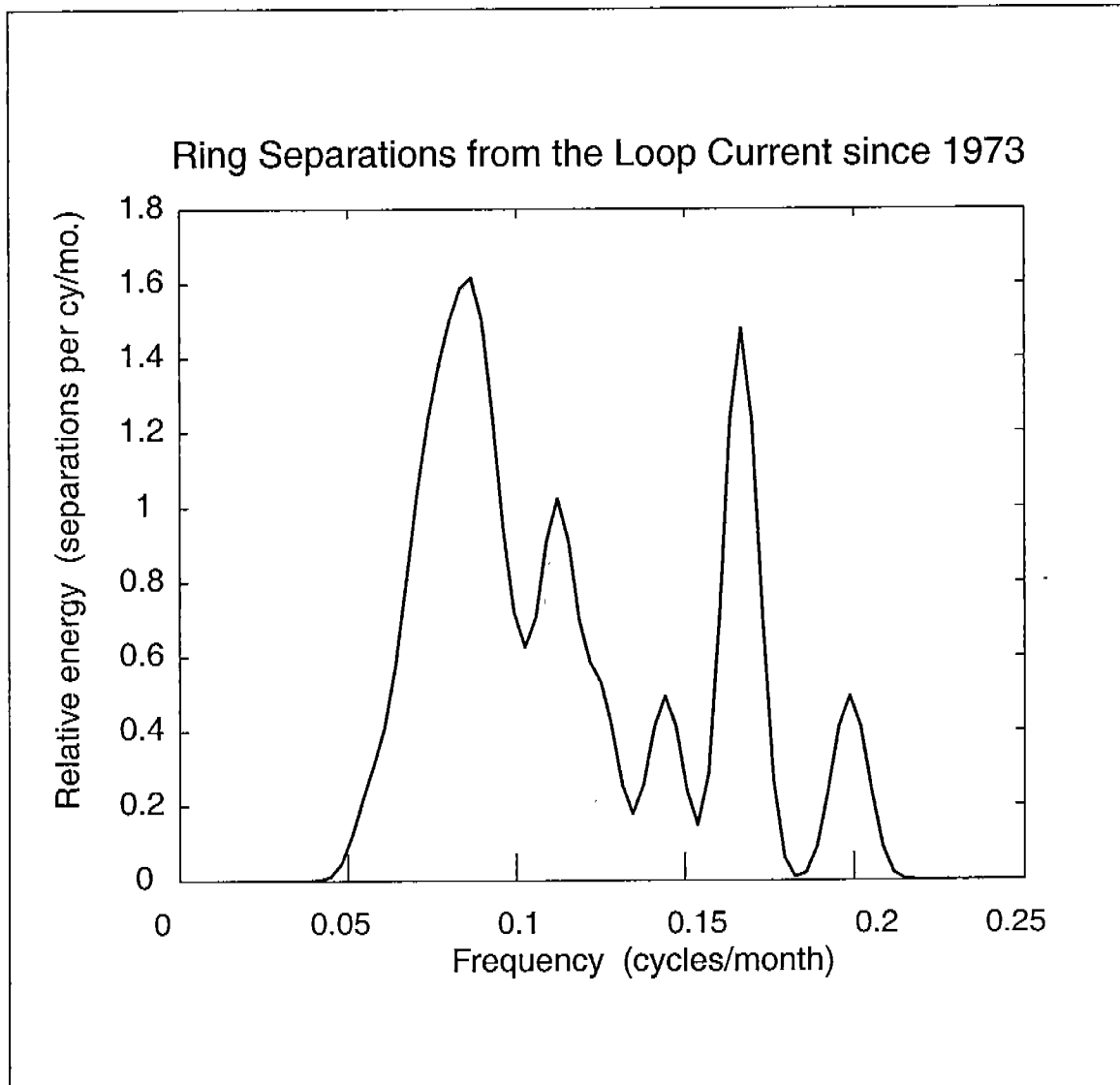


Figure 3.3-1. Periodicity of ring separations from the Loop Current. This figure is actually a histogram, plotted to resemble the usual power spectrum; both scales are linear. All known separations since July 1973 - Aug. 1999 are included. The original histogram has been smoothed by 5 Hanning passes. A single value at (3 mo) is omitted for clarity, and is offscale. Confidence limits of 80%, are obtained by multiplying (or dividing) any value by 1.7; determined by a bootstrap technique.

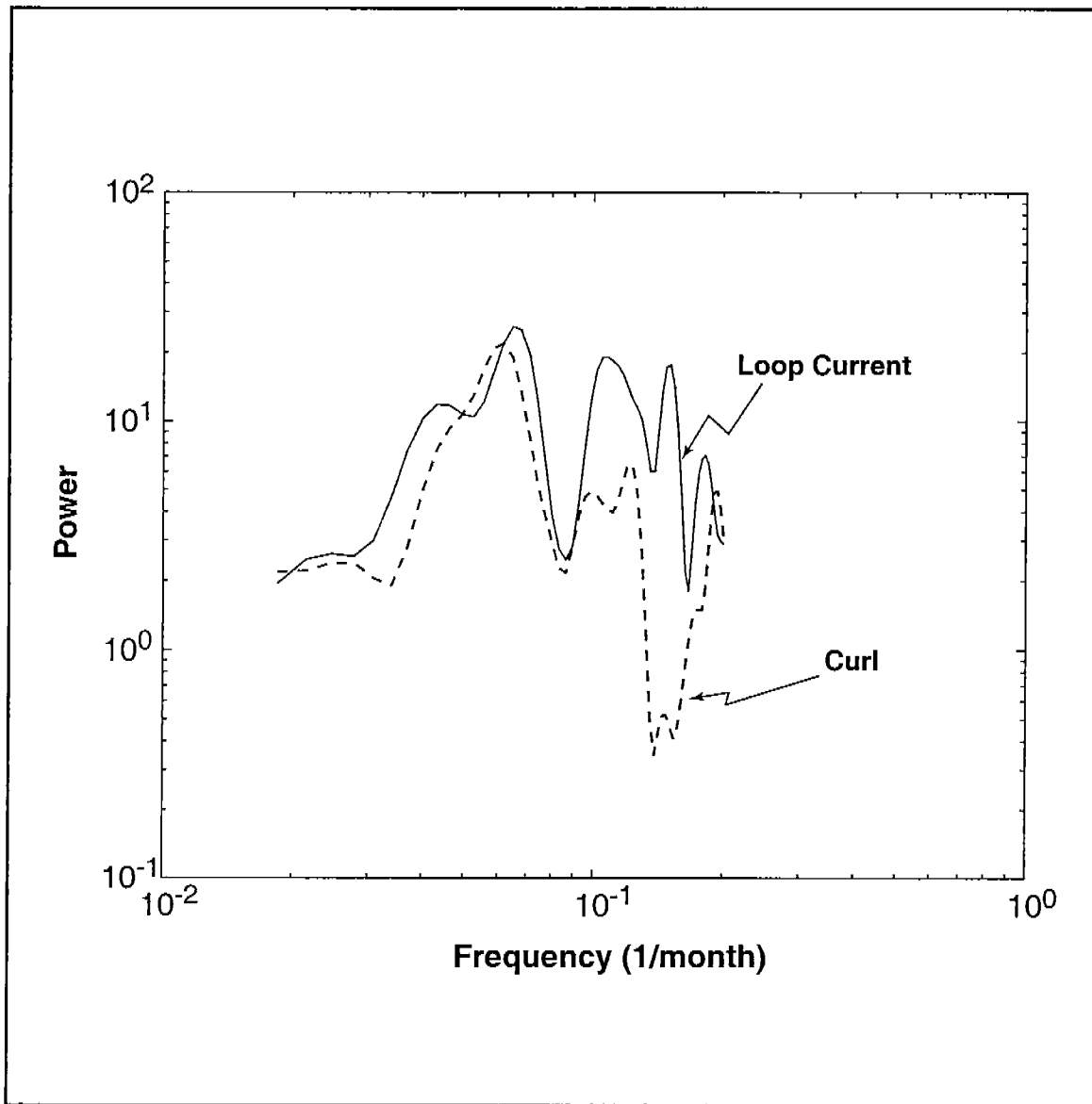


Figure 3.3-2. Power spectra of the north-south motion of the Loop Current and of wind stress curl over the full Gulf of Mexico. The Loop Current signal is from the time derivative of the northern-most position of the Loop Current front, from a variety of data sources. The wind curl is computed from the NCEP reanalysis wind data over the Gulf of Mexico plus a small region south of Yucatan Channel and west of Cuba. Smoothing is by 5 Hanning passes. The mean annual cycle of the curl was removed from the signal before computing the spectrum. The monthly data begin in July 1973.

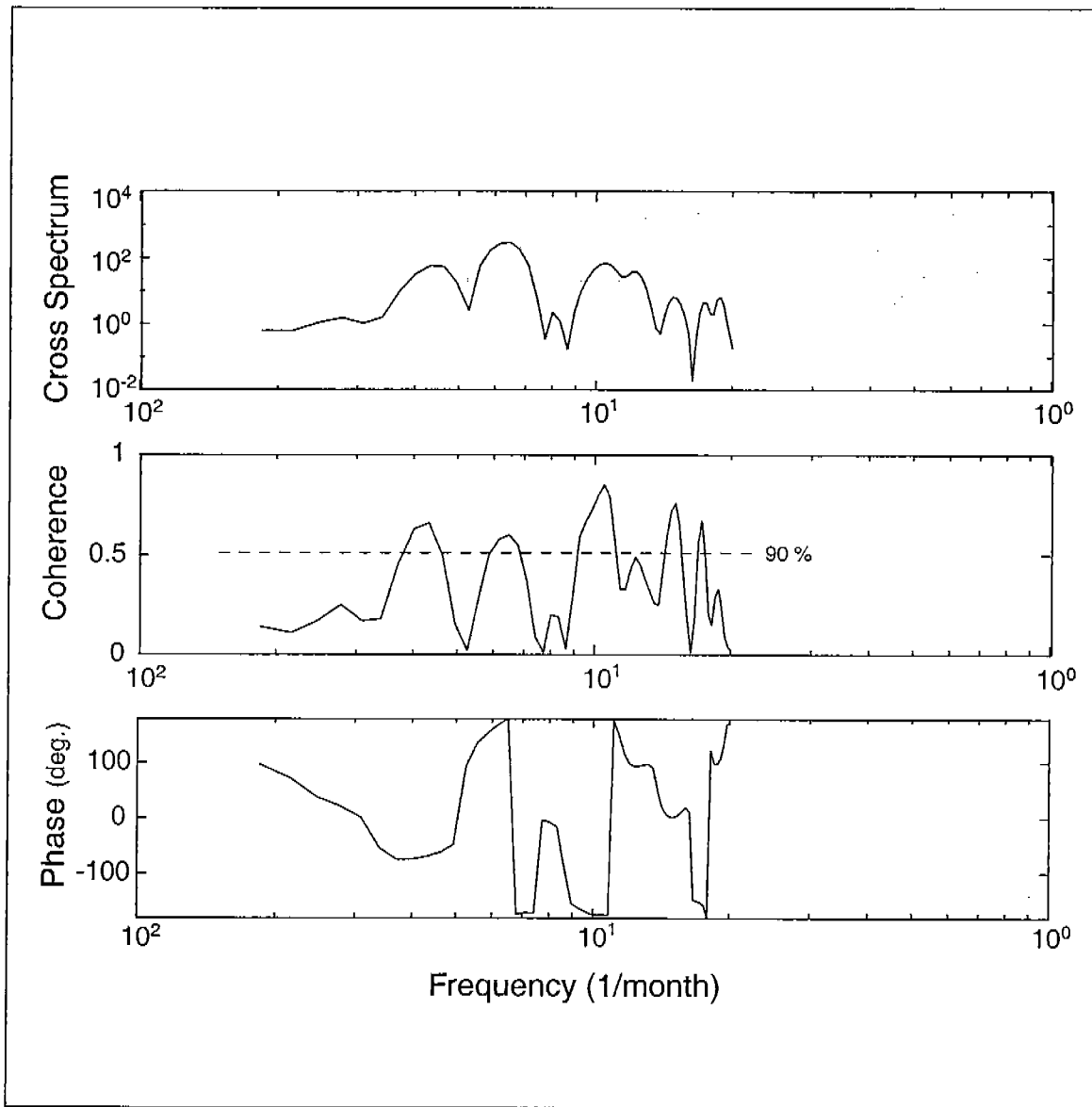


Figure 3.3-3. Cross spectra between the wind curl and Loop Current variability. The upper panel shows cross spectral power; middle panel, coherence squared, and lower panel phase. Smoothing is by 5 Hanning passes. The 90% confidence limits are shown.

4.0 SLOPE CIRCULATION PATTERNS

4.1 Introduction

A detailed examination and description is provided of the vertical and horizontal patterns of currents over the slope, from the shelf break into the deeper water of the mid- and lower slope. Patterns are complex, having time and space scales covering a broad range. As developed, it is clear that a eddies, both anticyclonic and cyclonic, have a substantial influence on observed current patterns.

4.2 Types and Sources of Eddy Influences

4.2.1 Loop Current Frontal Eddies

A variety of differing types of eddy features were seen to affect the circulation patterns documented by the in-situ observations, the ship-based surveys and the satellite remotely sensed observations. Of particular relevance are LC frontal eddies (LCFE) that form on the boundary of the LC and on the boundary of LC rings. A LCFE is an essentially cyclonic feature that forms along a boundary. They have describe and documented extensively along the Gulf Stream and to a lesser extent along the LC but along the west Florida escarpment. The LCFE affecting the northeastern Gulf can be much larger than those along the west Florida shelf/slope due to the lack of a proximate constraining boundary. An example of a LCFE is shown in Figure 4.2-1. The cyclonic/counterclockwise flow is indicated by an arrow. As is often the case, a trailing filament of warmer water extends out from the LC or ring in advance of the cold core cyclonic eddy. These features move/migrate along the frontal boundary and evolve as they move. The filaments can extend further. At times, the filament can become almost detached from the frontal boundary and end up a relatively thinner lens of warmer water ballooning out from the frontal boundary. The warm filament/streamer can extend the influence of the LC frontal boundary well away from the actual position of the main LC boundary.

The cause of the frontal boundary features is a topic of open discussion. On the Gulf Stream warm/western wall, the filament is associated with the crest of a migrating wave motion and the cyclone associated with the trough of the wavelike oscillation. Such associations are not so readily resolved along the LC, however, the similarity between the features would suggest similar causes that remain to be well defined. The presence of LCFEs along separated LC rings points to the role of stability of the frontal boundary as a contributing factor in their formation and evolution.

As might be expected, the potential direct influence of LCFEs within the present study area is greater when the LC is well extended to the north. In contrast, the influence of frontal eddies on rings are associated with the local presence of a ring, prior to having migrated westward out of the eastern Gulf. The specific influence of the various component elements of a LCFE (cold pool, filament, etc) depend on factors such as the location relative to instrument and bottom topography, the distance

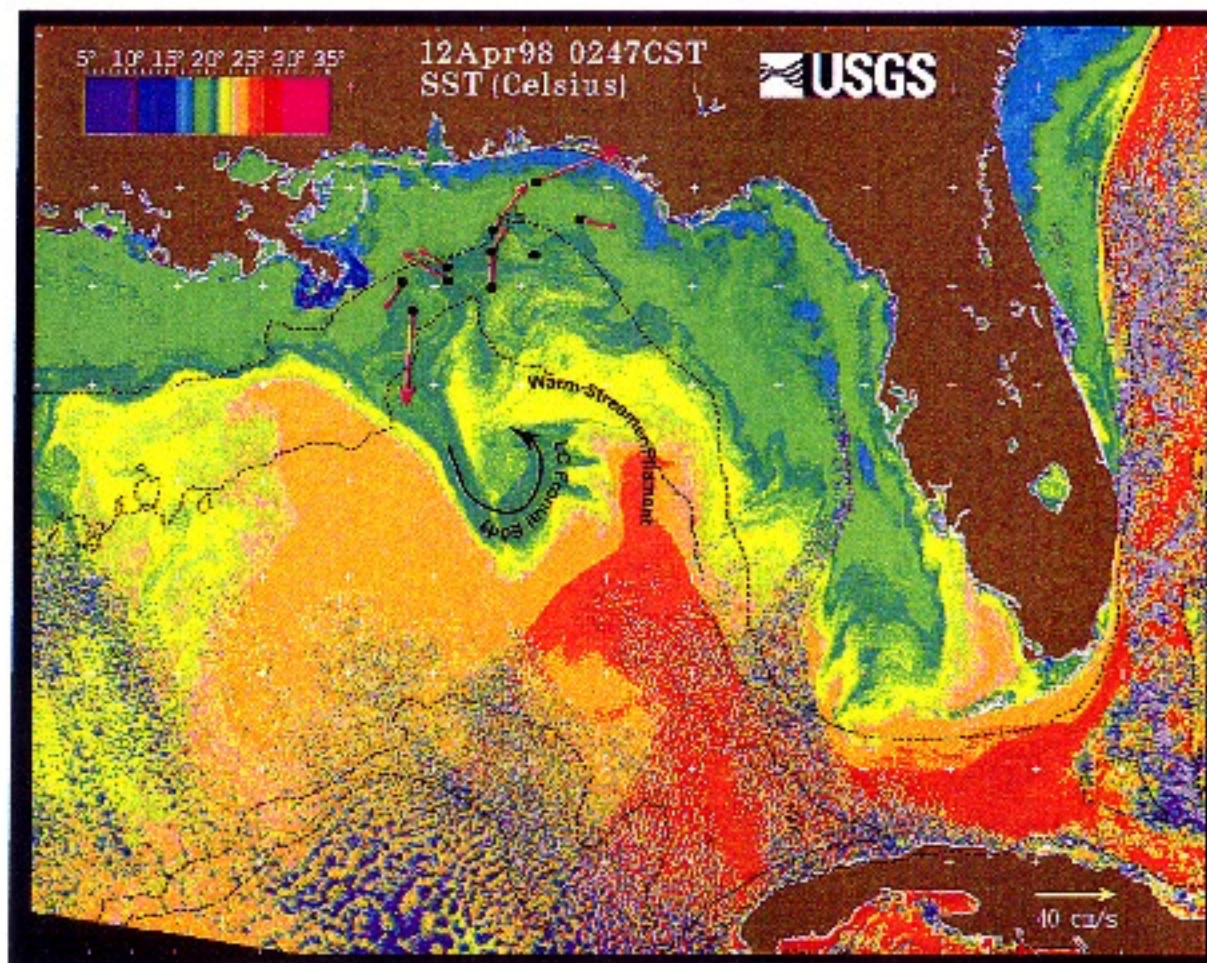


Figure 4.2-1. SST image for April 12, 1998 (0247 CST). Measured current vectors are overlaid on the image in the study area. Features mentioned in the text have been labelled for clarity.

from the study area to the frontal boundary, the presence or absence of other dynamic features in the region.

Clearly, it is not possible to develop a one or two scenarios of the influence of LCFE on conditions in the study area. An effort has been made to conceptualize the influence of LCFEs by developing a series of "modes" that describe the patterns identified during this study.

- **Mode 2a.** One of the more common events causing strong flow and temperature variability within the moored array comes from the interaction of LCFE's with the slope. Mode 2a represents the interaction that occurs from LCFE's moving around the northern boundary of a mature (northward extended) LC. This process is shown schematically in Figure 4.2-2. LCFE's can have horizontal scales of several hundred kilometers and extend to depths of 600 to 800m. The cyclonic circulation in these features entrains warm LC water around their cold cores in the upper 100m. As the eddies move to the east around the LC and south of the array, they leave a long trailing warm streamer of upper level LC water that extends into the moored array. Isobaths curvature in the array shifts from a east-west orientation in the western part to more SE-NW alignment in the eastern part of the array. Thus, the northwest extension of a warm streamer will cross isobaths into shallower water. As a result the warm upper layer will shrink and vorticity constraints will cause an anticyclonic rotation. The streamer continues to pump warm water into the array region as the LCFE moves to the southeast causing the eventual spin-up of a warm anticyclonic eddy over the array. This produces an eastward flow with a negative cross-slope temperature gradient in the upper 100m of the array. Below that depth, the cyclonic circulation in the LCFE causes strong, persistent westward flow. A number of LCFE's produced this type of current and temperature response during their passage south of the array. An example in SST imagery are given in Figure 4.2-3. Intrusions of these warm streamers can sometimes result in strong up-canyon flows in the DeSoto Canyon. Offshore flows can result from the convergence of the trailing wake of a LCFE with an approaching ring or LC crest. Both processes can result in significant cross-slope exchange.
- **Mode 2b.** Mode 2b is essentially the same as Mode 2a except the LCFE is located on the boundary of a LC ring south of the array instead of the LC itself (Figure 4.2-4).
- **Mode 2c.** Mode 2c occurs when a LCFE is located close to the array and is directly interacting with the slope (Figure 4.2-5). The warm streamer is more parallel to the slope bathymetry and is advected to the west around the cold core of the eddy. As a result the flow is westward throughout the array both above and below 100m.
- **Mode 2d.** Mode 2d represents the type of flow interaction that can occur from a LCFE on the eastern boundary of a warm ring, where its southward movement is blocked by a growing LC (Figure 4.2-6). The LCFE produces westward flow in the deeper waters below 200m

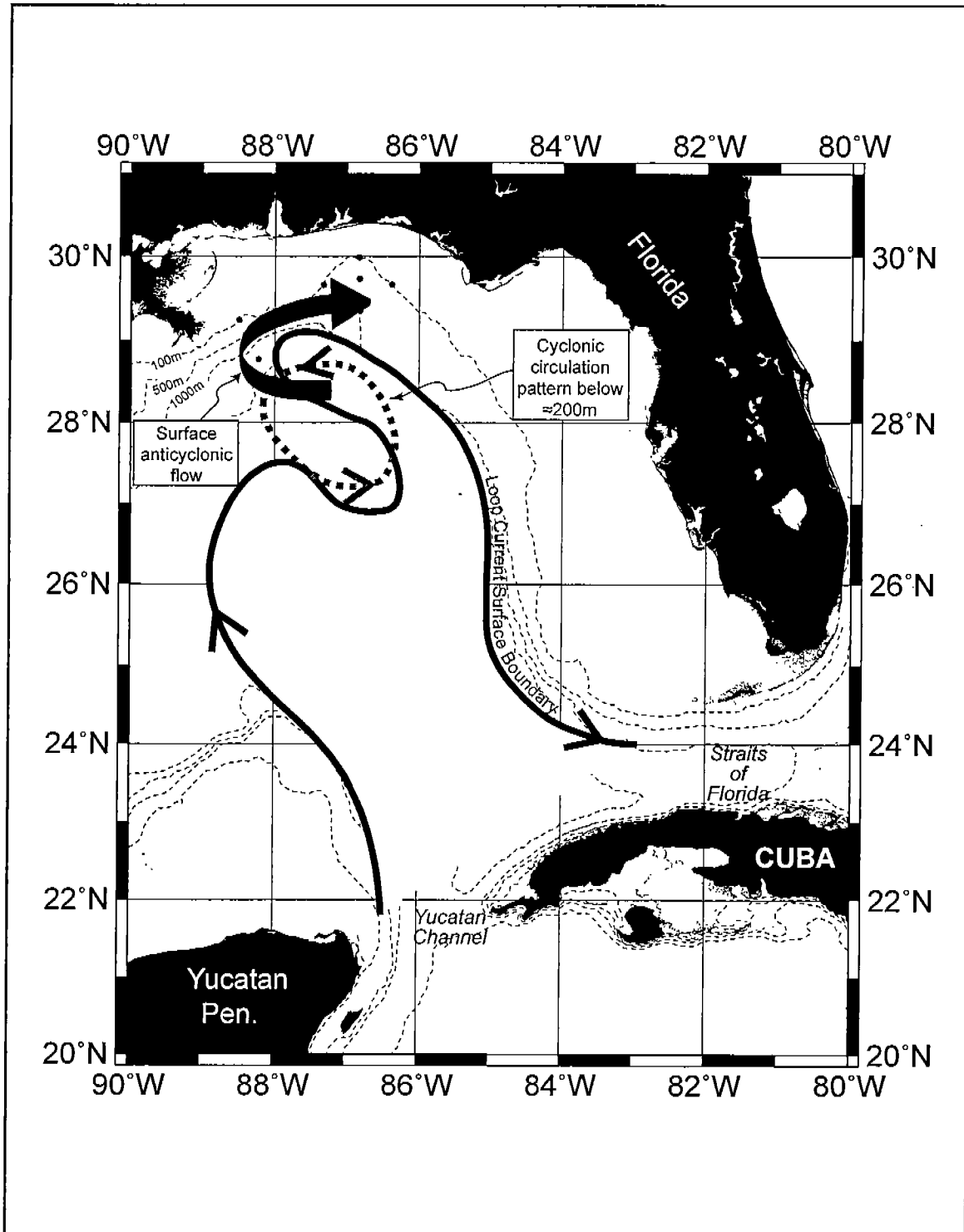


Figure 4.2-2. Conceptual model of a Loop Current frontal eddy flow interaction with the slope in the study region.

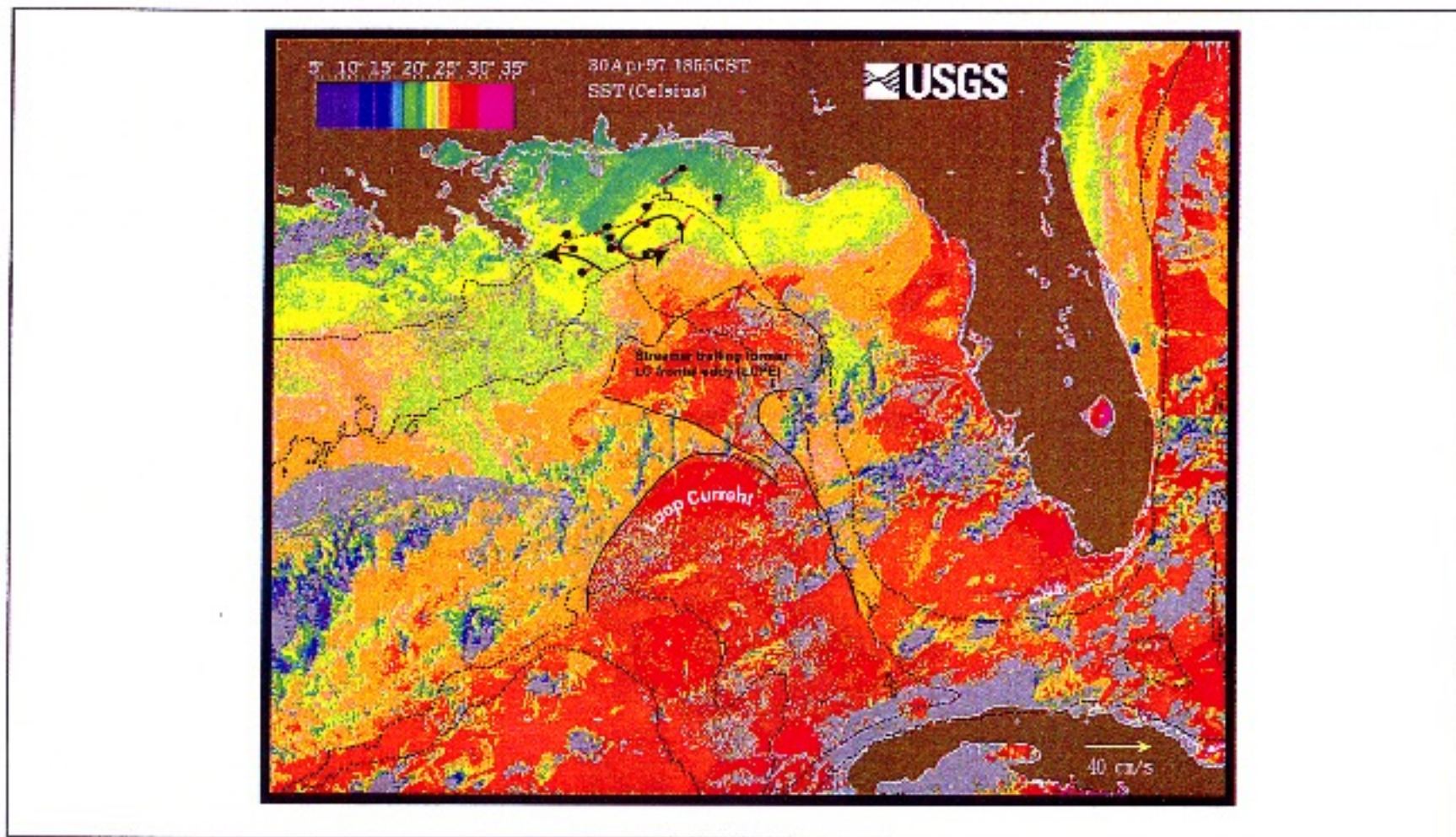


Figure 4.2-3. SST image for April 30, 1997 (1355 CST). Measured surface current vectors are overlaid on the image in the study area. A streamer trailing a former LC frontal eddy is labelled, as is the Loop Current proper.

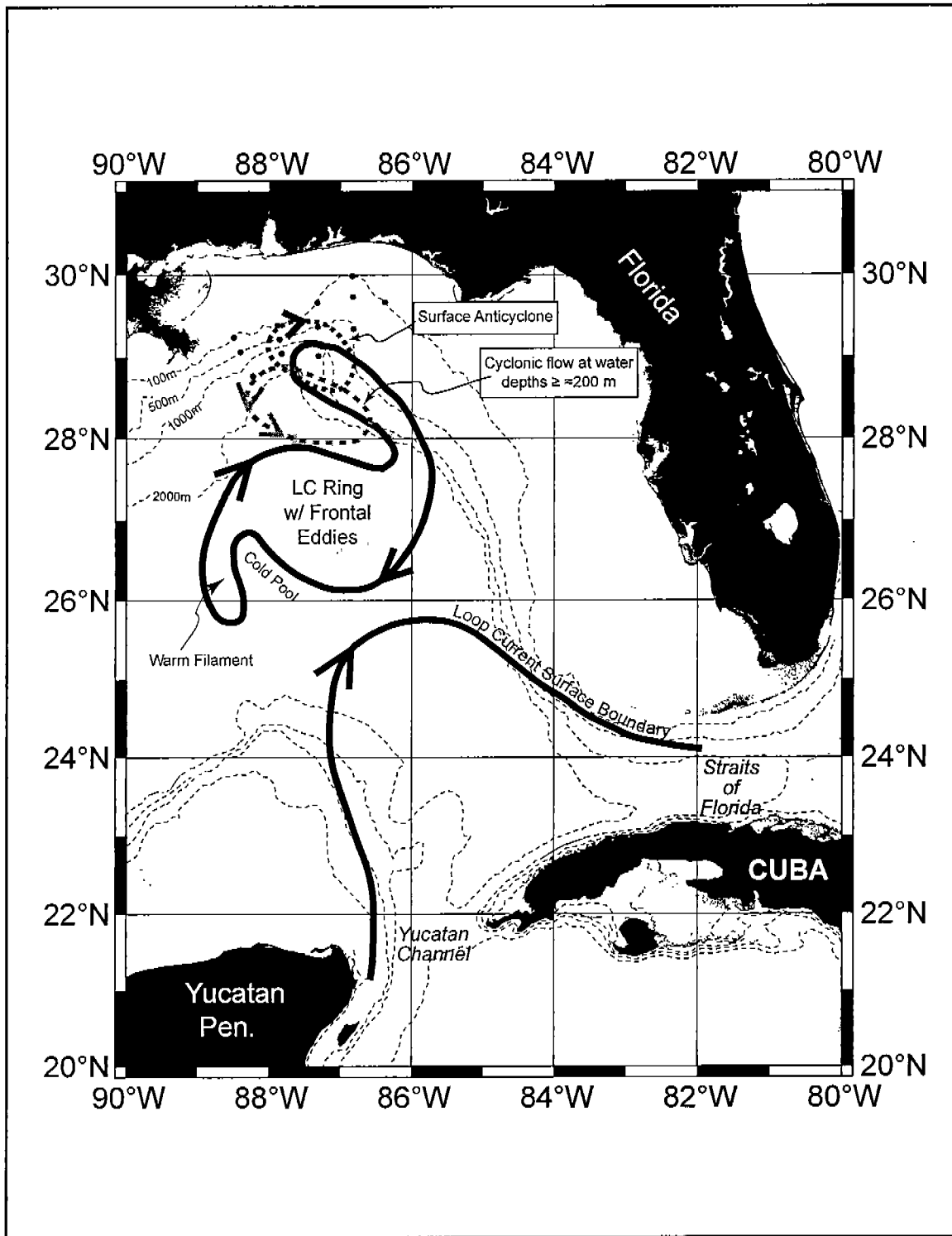


Figure 4.2-4. Conceptual model of flow interaction with the slope in the study region from a LCFE on the boundary of a warm LC ring.

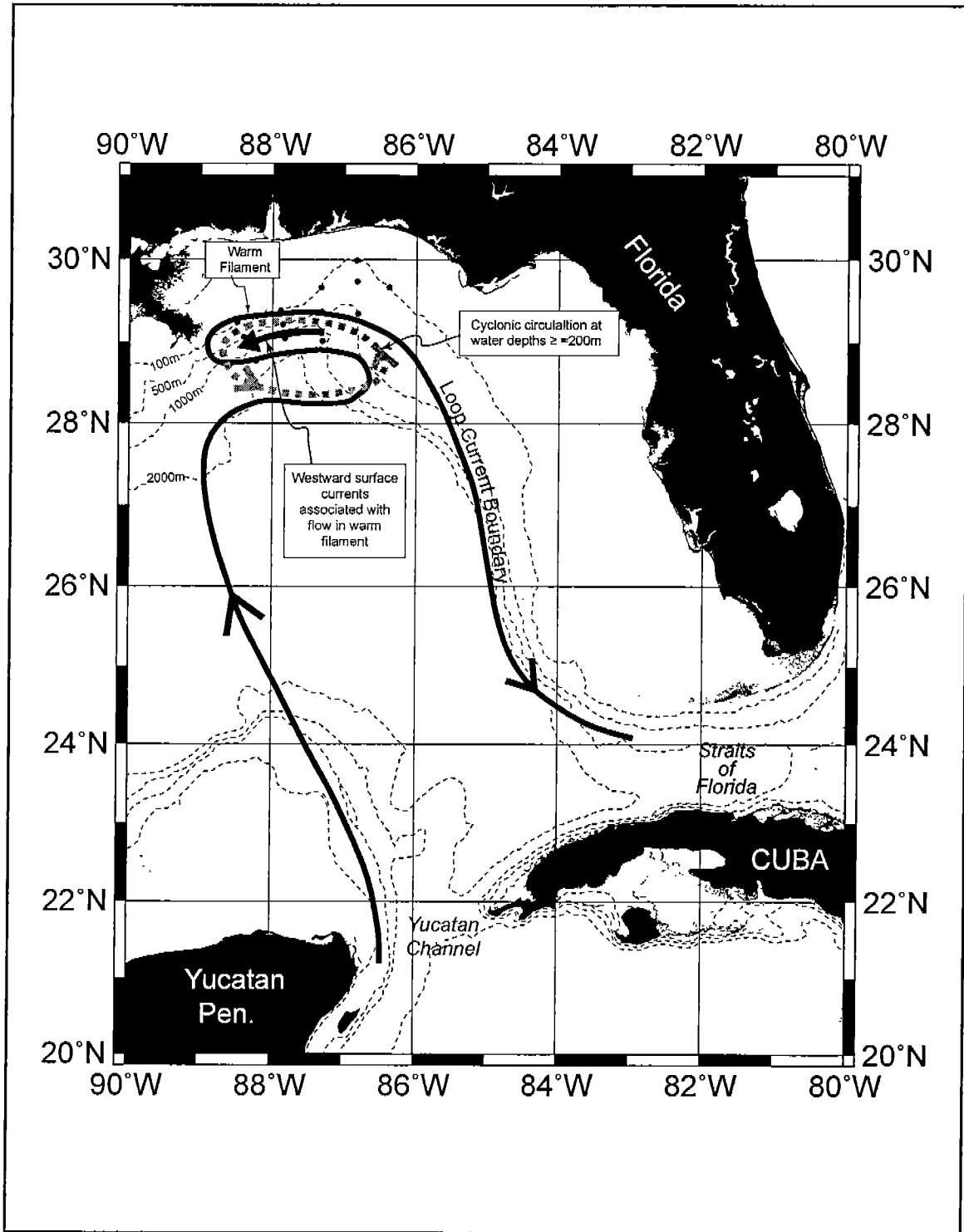


Figure 4.2-5. Conceptual model of flow interaction with the slope from a Loop Current Frontal Eddy close to the study region.

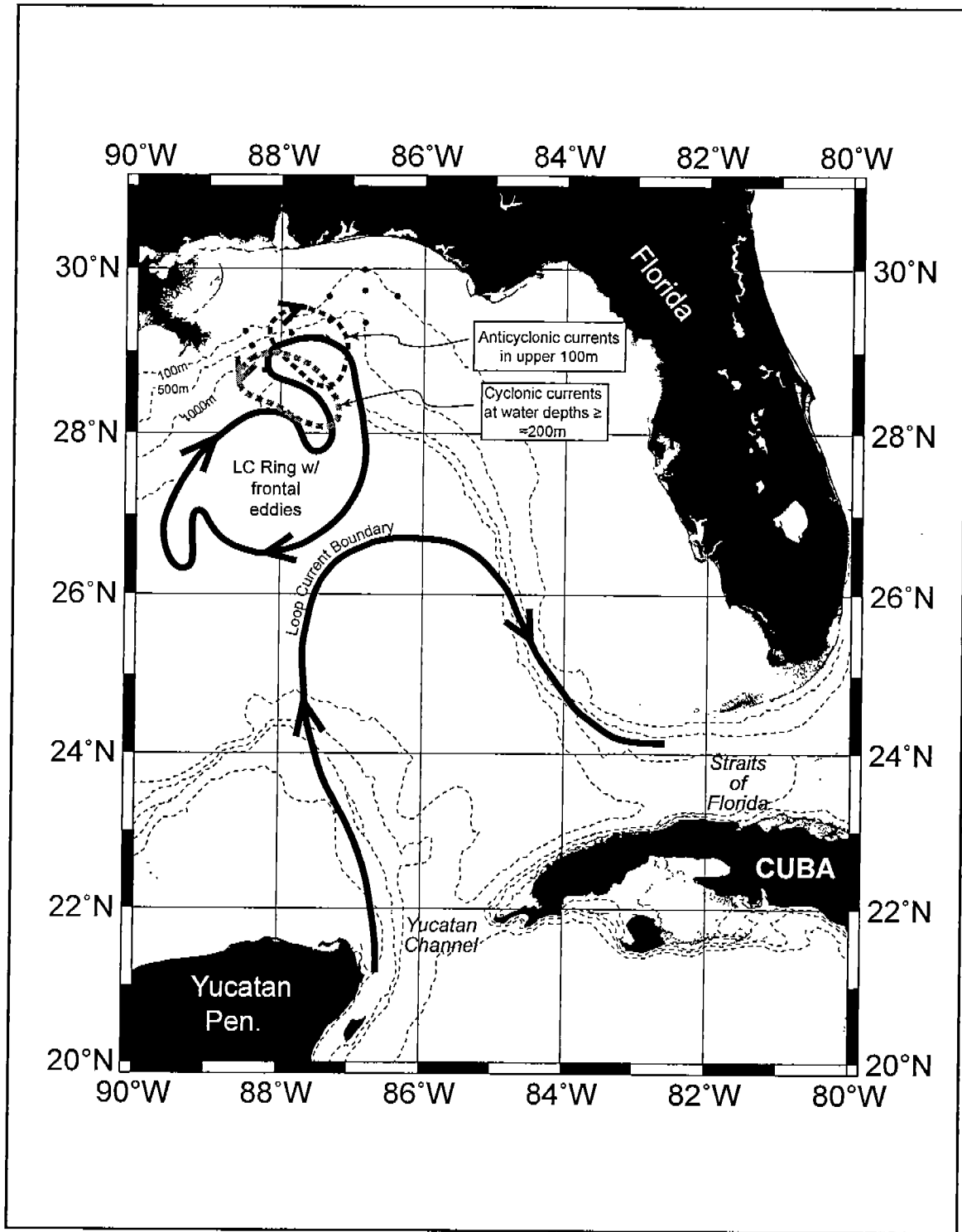


Figure 4.2-6. Conceptualization of flow interaction with the slope from a LCFE on the boundary of a warm LC ring located south of the Mississippi Delta and blocking the LC.

and eastward flow results in the upper 100m from the anticyclonic eddy that spins-up over the array from the warm streamer. Blockage of the movement of the LCFE can result in a near stationary eddy and prolonged influence on the flows in the study region.

4.2.2 Cyclonic and Anticyclonic Eddies

Remote sensing helped identify eddy like features that do not have a direct link to the LC or a LC ring. This is not to say that these features did not evolve as features in some way due to the LC as a source of energy and momentum; however, at the time they are identified this possible linkage is not readily apparent. Both cyclonic (counterclockwise) and anticyclonic (clockwise) rotating features were documented during this study and an effort was made to resolve their nature and influence. The horizontal scales of these features with both senses of rotation are comparable. Due to limitations in horizontal scale resolution with altimetry, the lower eddy diameter is smaller than can be well resolved by available altimetry. The upper length scale is on the order of 100 - 200 km.

These features evolve with time and migrate. The specific evolutionary course as well as the path and rate of movement are often dependent on the location and types of other features which surround the specific feature. Thus, there is not a common pattern for these features, rather the specific influence is described on a case-by-case basis. As determined from ship-survey data, currents in the upper layers and mid-to lower layers (500-1000m geostrophic velocity) can be in the opposite along shore directions. (Figure 4.2-7). Examples with no reversals with depth are shown in Figures 4.2-8.

4.2.3 Mean and Varying Circulation Patterns

Long-term (two year) mean current patterns were quite robust. Subdividing the records into two separate 12-month intervals produced results similar to the complete two-year record. In all cases the standard deviations were substantially larger than the means which points to the inherent importance of the variable flow patterns occurring in the study area. Near surface mean flows generally had an eastward component while below 70m, westward means occurred. Even such long-term averaging maintained a distinct counter current at depth. Superimposed on the means are long term but variable current and temperature patterns. Throughout the study, several intervals with durations of two months or greater of relatively sustained or persistent conditions (events) were identified (Figure 4.2-9). Averages and variances for each of these events were computed to characterize conditions during each event. The events represent a "mixed" event with cyclonic and anticyclonic conditions (S97), a cyclonic event (C) and an anticyclonic event (A). Very low frequency variability may indicate the presence of propagating topographic wave motions. This analysis also indicated to variance that was unexplained by low frequency EOF analyses, which pointed toward higher frequency, shorter scale motions as a possible source for a substantial component of the observed variability.

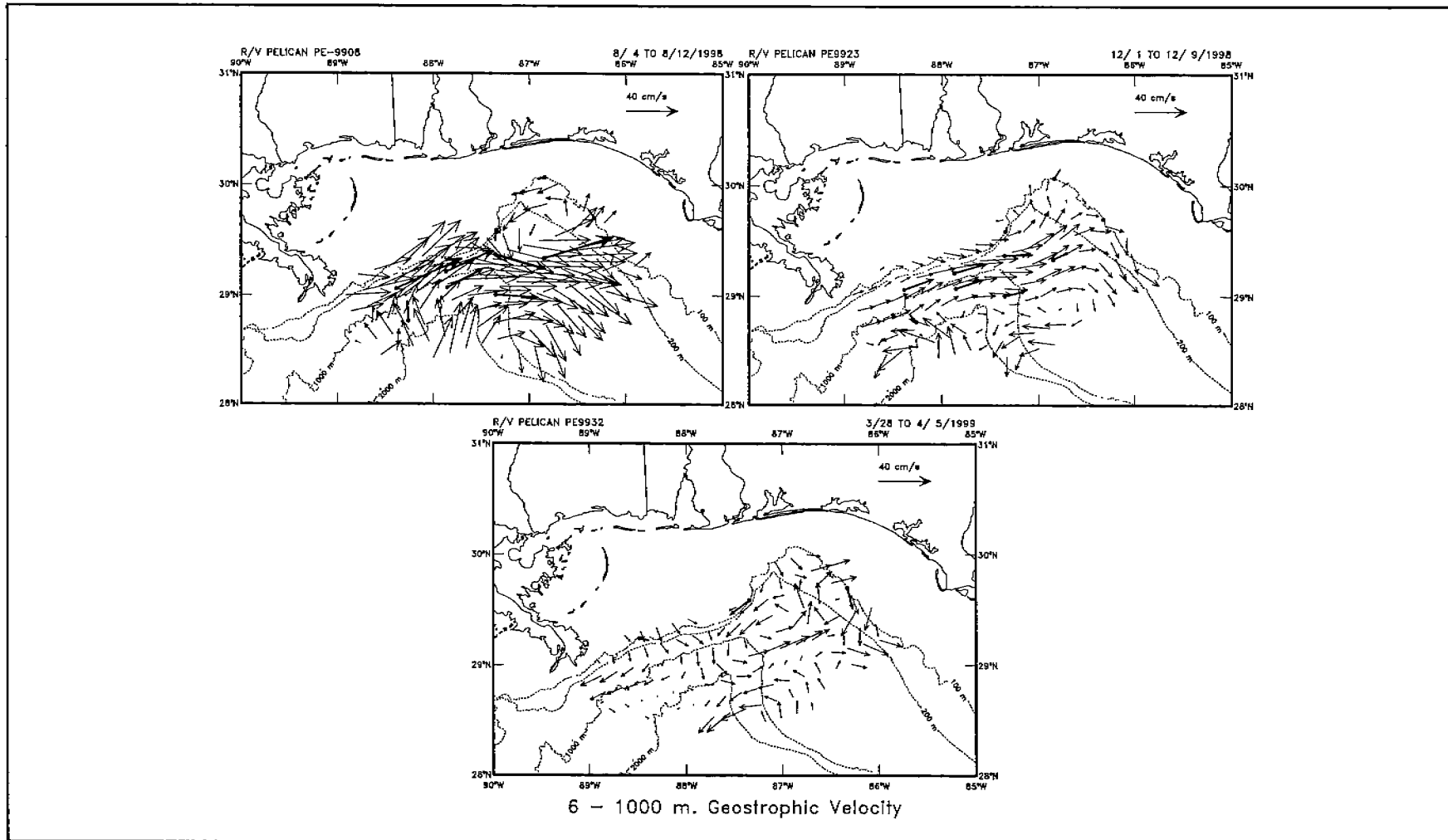


Figure 4.2-7. Geostrophic velocities at 6m from the hydrographic surveys. 5-day average velocity vectors (heavy arrows) from the 8m depth of the ADCP's are shown at stations marked with a dot.

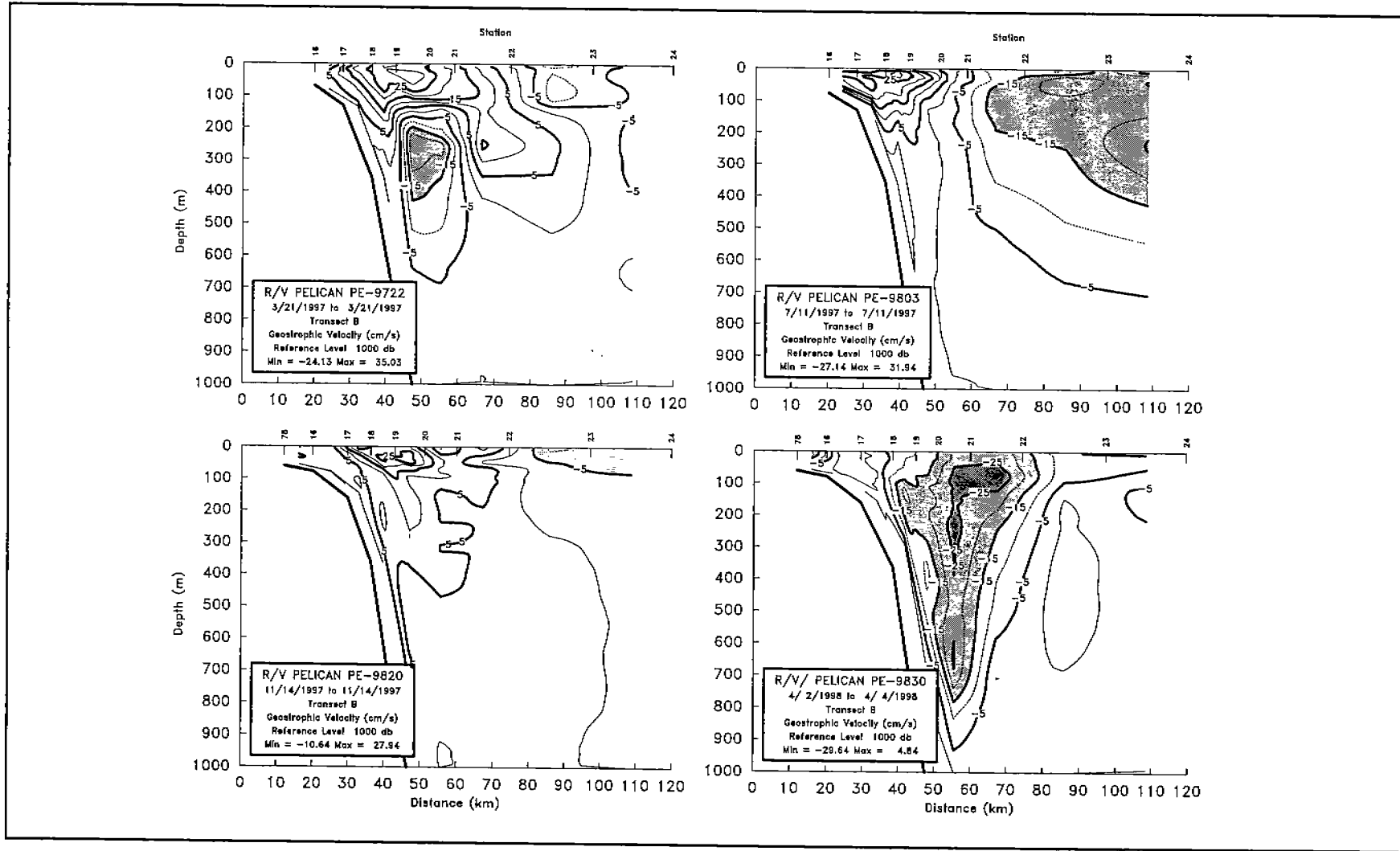


Figure 4.2-8. Geostrophic velocities on Section B for the indicated surveys. Positive velocities are eastward, normal to the section. Higher westward (negative) velocities are shaded.

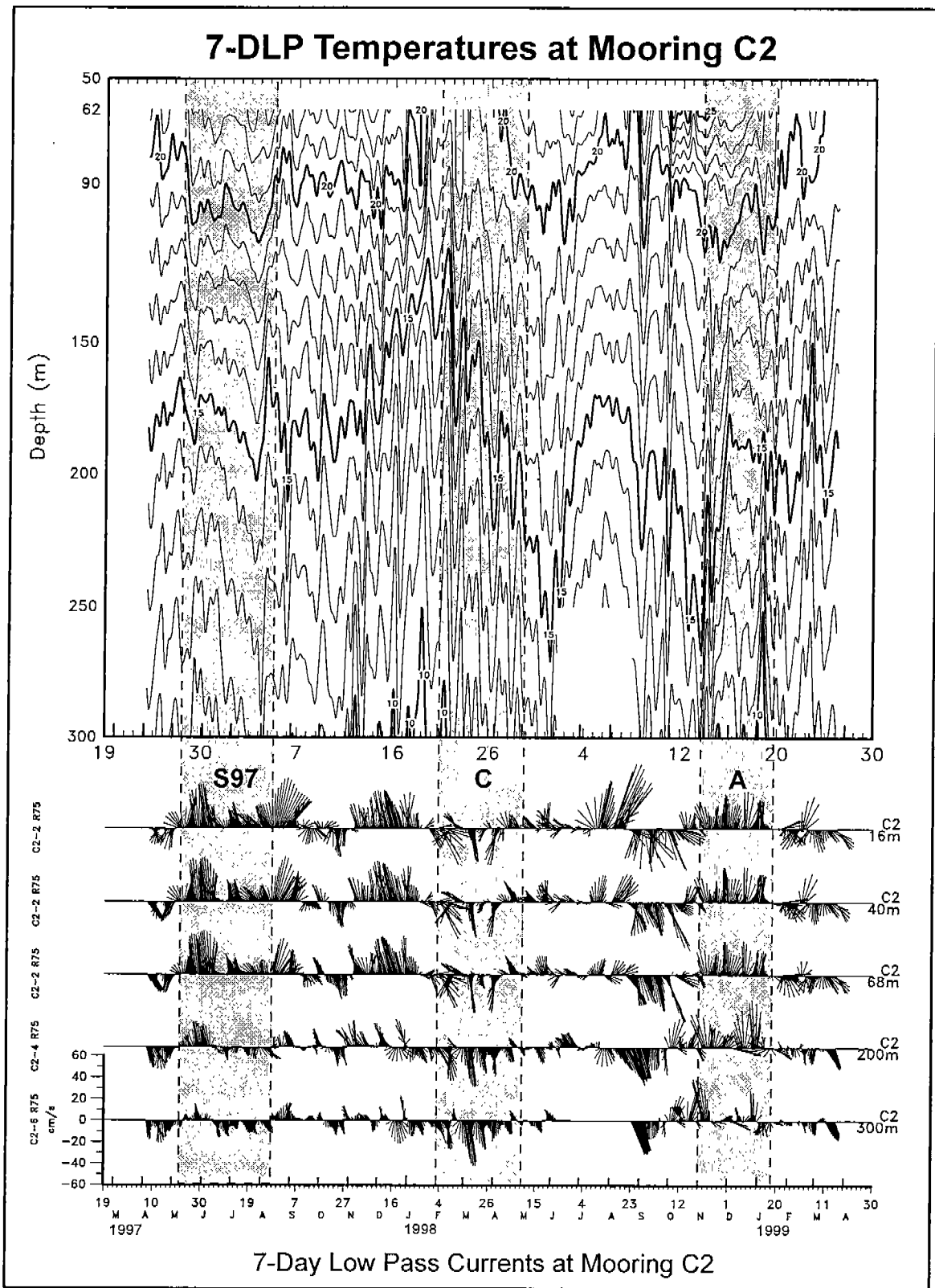


Figure 4.2-9. Seven-day low pass current vectors and isotherm depths for the upper 300 m of C2. Vectors pointing vertically upward are directed along isobath with an easterly component

4.2.4 Slope Dynamics and Fluxes

Vorticity over the slope appears to be in part dependent on the presence of eddy-like features, their location and sense of rotation. Because of the differing sense of rotation of cyclonic and anticyclonic eddies, it might be expected that the sign of the vorticity at the various slope locations was dependent on the above factors. It was not possible to develop a complete explanation that related vorticity to all specific velocity records. Some insights remain to be developed.

Momentum flux over the shelf break was governed by the influence of slope eddies and storm events. Eddies generally transferred momentum onshore onto the shelf from the slope and by this method slope processes affected the circulation patterns on the shelf. Although the rate of transfer was not as great as that occurring in substantial storms, the transfer due to eddies could persist for longer periods of time. Hurricanes created significant spikes in the momentum flux across the shelf break.

Heat and salt flux calculations were limited by placement of appropriate sensors. However, from the available data, it appears that eddies played a relatively minor role in the total flux of heat (0.1-2%) and salt (4-14%). The available data did indicate a strong correlation of salinity and temperature which was sufficient for temperature to be a surrogate for salinity. Consequently, water mass flux calculations may be computed from temperature and velocity alone.

Results of computations indicated that at some stations, mean fluxes across the shelf break were significant, while at others they were not. These results suggest that, over the long term, the water mass exchange may be something of a two-layer phenomenon with onshelf flux near the surface and offshore flux near the bottom. Results also suggested that wind-forced flows may have accounted for a significantly greater proportion of the cross-margin temperature flux near the bottom than at the surface. At all moorings, the largest cross-margin heat/temperature fluxes occurred during Hurricanes Earl and Georges.

4.2.5 Deep Currents

Previously, circulation in the upper 500m has been discussed. Over the mid- to upper slope, circulation was dominated by eddies and an eastward flowing current with reversed flows at depths below about 200m. The primary source of energy for these flows is the LC and LC rings/eddies which extend down to 800-1000m. It is about this depth that a relative minimum in kinetic energy occurs. Below this, motion does not correlate well, i.e. are not directly coupled with those higher in the water column. Deeper currents may be related to wave motions that could be related in some way to the LC and the separation and migration of LC rings. Observations did not provide information that was sufficient to explain the apparent wavelike motions measured by the deepest current meters on the 1300m moorings.

5.0 ATMOSPHERIC FORCING

5.1 Synoptic Scale Forcing

Shelfbreak and upper level slope currents had a significant response to coherent synoptic-scale wind events. Alongshelf winds that were coherent over the shelf domain generated cross-shelf transports in the surface layer with opposite return flows beneath. The geostrophic adjustment time for sea level to balance alongshore flows is approximately two hours. Time for the along shelf currents to reach equilibrium with the along shelf wind stress was about 28 hours. The separation of the periodicity of eddy forcing (greater than 20 days) and synoptic wind forcing (5 to 15 days in winter) facilitates to some degree an examination of these two mechanism.

5.2 Seasonal Wind Response on the Slope

Because the transition seasons of spring and fall are short and often not well defined in the Gulf, two winter and two summer seasons were partitioned and used to examine seasonal scale forcing of slope circulations. The winter seasons typically have the more vigorous forcing due to wind stress in the 5-15 day period band of synoptic scale events.

In this portion of the northern Gulf, these winter atmospheric events are low pressure systems and fronts that move over and through the northeastern Gulf of Mexico. The interval between events can vary within a winter season with the shortest interval often occurring in the heart of the season. Results indicate that there was a strong slope current response to winds in the two summer seasons. During the two summer seasons, there was no significant coherence between the along- and cross slope wind stress modes and the principal velocity modes for the shelf break and upper slope moorings.

It is difficult to partition eddy influences from those forced by wind stress. The relative influence of wind forcing in summer was dependent on the relative strength of eddy-driven motions. During both summers, eddy influences were strong and the mean flow was toward the east. Fluctuations in along isobath currents enhanced or opposed this mean motion. Some of the variability due to atmospheric processes was difficult to distinguish from eddy effects in the same frequency band.

In the two winters during which current measurements were made, variability of the primary EOF modes generally followed the trend of the isobaths. As during the summers, slower underlying variability occurred due to eddies, however, more energetic fluctuations having shorter periods (on the order of three to ten days) were associated with atmospheric forcing. The visual correlation of this higher frequency variability suggests that the longer period fluctuations associated with eddies caused a reduction in the correlation between modes. During winter, at those frequencies where wind stress EOF modes have energy, the coherence between wind stress and current modes was high. The phase differences show that the wind stress modes led the currents modes by 1 to 2 days.

5.3 Canyon Response to Hurricanes

During these field measurements, two hurricanes (Earl and Georges) moved over portions of the in-situ instrument arrays. This provided an opportunity to examine the oceanographic response of the DeSoto Canyon to at least these two exposures to extreme atmospheric forcing. Because the storm intensity varied, as did the extent of the associated wind field and the path, the oceanographic response differed to some degree between the two storms.

Both hurricanes generated strong along isobath flow near the surface with currents being somewhat stronger during Georges. Strong and variable cross isobath flows were seen at the canyon edge during both storms. During Earl, highest velocities at the canyon edge were in a near surface jet. During Georges, high velocities extended throughout the water column with a mid-depth maximum of along isobath velocity in the vicinity of mooring C1.

An examination of volume flux during these storms indicates that Georges caused significantly (several times) greater cross-isobath transport at the shelf break than did Earl. The excess onshore transport over the passage of the storm points to greater offshore transport at a location not documented with measurements.

Several prior studies have documented the inertial current response to strong storms passing over the slope. The inertial response of interest results from the relatively quick (relative to oceanographic adjustment) impulse being provided by the combined influence of a migrating wind stress field on the surface and the migrating oceanographic pressure dome under the hurricanes. After the input of momentum at the surface, the resulting motion is controlled by the Coriolis force that causes circular like motion of the water particles with a periodicity governed by the magnitude of the Coriolis force, which is dependent on the latitude. In this study area at approximately 29°N the inertial current period is 24.75 hours or 0.97 cycles per day. This motion propagates downward in the water column, so the phase and magnitude of currents at the surface can differ from those occurring at various depths.

The inertial current magnitudes following passage of these two hurricanes varied considerable between mooring/locations. The strongest inertial currents associated with Earl occurred near the surface at mooring C3 in 1300m of water (Figure 5.3-1). For both storms, relatively weak inertial currents were seen at the shelf break; stronger currents occurred in the interior of the DeSoto Canyon. There is some evidence that the inertial current pulse may have propagated horizontally, arriving at locations further to the east at later times. In contrast and as shown in Figure 5.3-1, inertial current from Hurricane Georges did not display similar eastward phase propagation. The relative strength of the inertial response to hurricanes can be seen in Figure 5.3-2 that shows the amplitudes of inertial currents over the duration of the measurements at several locations and depths.

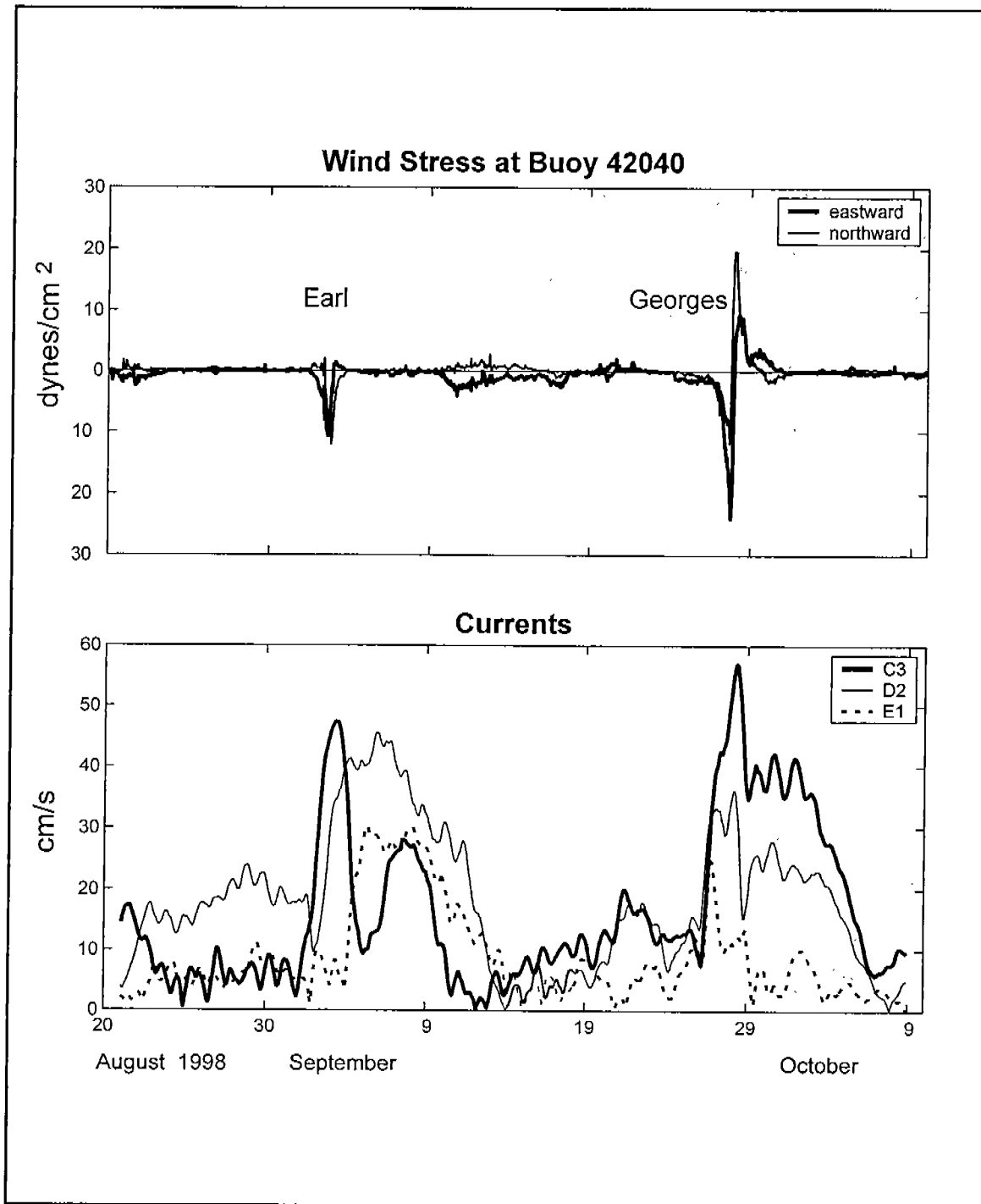


Figure 5.3-1. Comparison of inertial current magnitudes seen near the surface at moorings C3, D2 and E1 during late summer-early autumn 1998

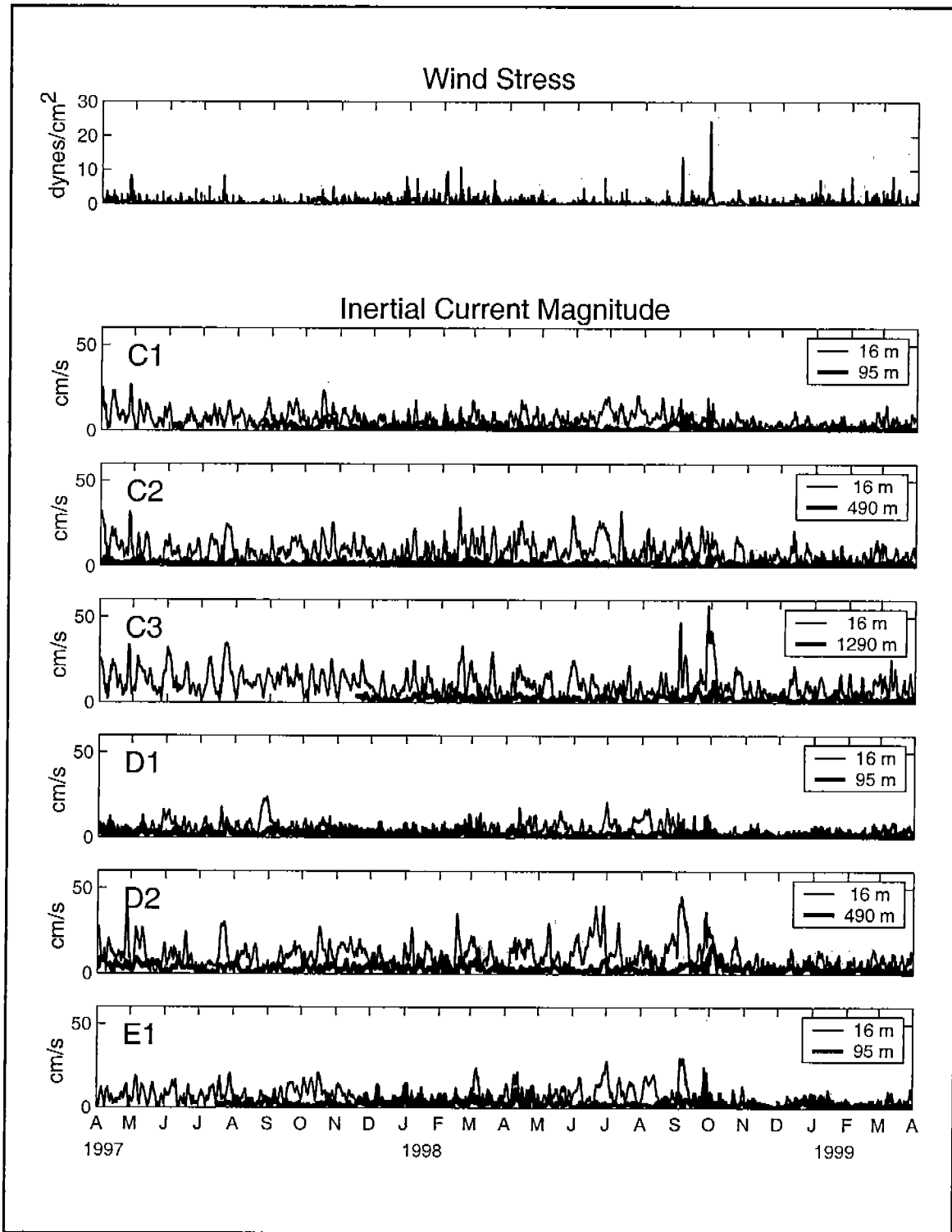


Figure 5.3-2. Surface wind stress together with near-bottom and near-surface inertial current magnitude observed at the indicated moorings over the study period. Because of gaps in the wind records, wind stresses over April 1997–November 1998 was computed from buoy 42040 wind velocities and subsequent wind stresses were computed using wind velocities from buoy 42039.

5.4 Non-hurricane Inertial Currents

As indicated above, the local inertial period is within the diurnal tidal spectral peak. To separate inertial motions from internal tidal currents relies on the regularity of the tidal signal and the lack of corresponding regularity of inertial currents. In addition, the internal tides should be phased locked over the vertical column, where as inertial currents will not have that vertical phase relationship.

The strongest inertial oscillations were at C3, the mooring furthest offshore. During the summer of 1997, inertial currents were present in spite of the weak wind speeds. Some initiation of bursts of inertial currents seem to have been associated with abrupt wind shifts. In contrast, during that winter when wind speeds were greater, inertial currents were weaker. The lack of vertical stratification at the shallower water sites can reduce the vigor of the inertial response. The argument is made that the vorticity associated with eddies and jets over the slope can trap offshore propagating inertial currents, and thus enhance the inertial currents at the deep water sites as compared to those at the shelf break.

These measurements show that non-hurricane inertial currents dominated the high frequency current fluctuations and were present in the offshore waters throughout the year. Their spatial structure was complex because of the characteristic intermittency and the velocity and vorticity structure of the upper-layer flows on the slope. This is in contrast to the Texas-Louisiana slope where the inertial energy decayed rapidly seaward of the shelf break.

6.0 SUMMARY

The DeSoto Canyon Eddy Intrusion Study established a comprehensive set of observations to evaluate and describe the oceanographic conditions within the study area. Each of the PIs effectively utilized multivariate data sets to isolate and describe often complex current and flow patterns. The availability of remotely sensed data, in particular SSH information, as well as ship-based surveys provided essential spatial and temporal extensions to the arrays of in-situ instruments that provided a nearly complete set of observations.



The Department of the Interior Mission

As the Nation's principal conservation agency, the Department of the Interior has responsibility for most of our nationally owned public lands and natural resources. This includes fostering sound use of our land and water resources; protecting our fish, wildlife, and biological diversity; preserving the environmental and cultural values of our national parks and historical places; and providing for the enjoyment of life through outdoor recreation. The Department assesses our energy and mineral resources and works to ensure that their development is in the best interests of all our people by encouraging stewardship and citizen participation in their care. The Department also has a major responsibility for American Indian reservation communities and for people who live in island territories under U.S. administration.



The Minerals Management Service Mission

As a bureau of the Department of the Interior, the Minerals Management Service's (MMS) primary responsibilities are to manage the mineral resources located on the Nation's Outer Continental Shelf (OCS), collect revenue from the Federal OCS and onshore Federal and Indian lands, and distribute those revenues.

Moreover, in working to meet its responsibilities, the **Offshore Minerals Management Program** administers the OCS competitive leasing program and oversees the safe and environmentally sound exploration and production of our Nation's offshore natural gas, oil and other mineral resources. The **MMS Royalty Management Program** meets its responsibilities by ensuring the efficient, timely and accurate collection and disbursement of revenue from mineral leasing and production due to Indian tribes and allottees, States and the U.S. Treasury.

The MMS strives to fulfill its responsibilities through the general guiding principles of: (1) being responsive to the public's concerns and interests by maintaining a dialogue with all potentially affected parties and (2) carrying out its programs with an emphasis on working to enhance the quality of life for all Americans by lending MMS assistance and expertise to economic development and environmental protection.